between these two groups. Similarly, significant reductions were detected in the bacterial density of mice nasally administered either PspA plus Pam3CSK4, Poly(I:C) or LPS, but not CpG1826, compared with mice nasally administered either PspA or PBS alone ($P < 0.05$). No significant differences were detected in bacterial density among mice nasally administered either Pam3CSK4, Poly(I:C) or LPS.

4. Discussion

In the present study, nasal immunization with PspA plus each TLR agonist, such as either Pam3CSK4, Poly(I:C), LPS or CpG1826, induced PspA-specific IgA and IgG in the airways as well as PspA-specific IgG in systemic circulation of mice. In contrast, nasal administration of PspA alone induced PspA-specific IgG in plasma, but neither PspA-specific IgA nor IgG in the airways. Therefore, we confirmed that each TLR agonist was an effective nasal adjuvant for the PspA antigen.

The concentrations of PspA-specific IgG in both BALF and plasma and PspA-specific IgA in both BALF and NW increased similarly in mice administered PspA plus each TLR agonist. Furthermore, Pam3CSK4 and LPS induced Th2-associated IgG isotype responses, while Poly(I:C) and CpG 1826 induced Th1- and Th2-associated IgG isotype responses. Previous studies also reported that both CpG motifs and Poly(I:C) induced a Th1 response: our data are consistent with these reports [26,32]. Moreover, the previous reports on the Th2 immune response induced by agonists of either TLR2 (Pam3Cys) or TLR4 (*lpxL1 mutant* LPS), are consistent with the results we obtained using either Pam3CSK4 or LPS [26,33].

It is of interest to determine whether the PspA-specific antibody induced in the airway by nasal immunization of PspA plus agonist of TLR has a protective role against pneumococcal infection. Arulanandam et al. demonstrated that intranasal immunization with PspA plus interleukin-12 (IL-12) induced the concentrations of PspA-specific IgG1, IgG2a and IgA in both plasma and BALF of mice, compared with administration of PspA alone [34]. Because IL-12 activates Th1 and NK cells to induce IFN-γ, the production of both Th1- and Th2-associated IgG isotypes specific for PspA were found in this study. Furthermore, the authors found that immune sera raised by PspA plus IL-12 augmented opsonophagocytic activity against *S. pneumoniae*. This response was primarily attributable to IgG2a and, to a lesser extent, IgA, although this assay evaluated antibody-mediated opsonophagocytic activity without complement. Because PspA-specific antibodies overcome the anti-complementary effects of PspA [11], in the presence of a complement, they likely mediate the efficient opsonophagocytic killing of *S. pneumoniae*.

In our sub-lethal pneumonia model using a serotype 3 WU2 strain, the significant reduction in bacterial density in the lungs of mice nasally administered PspA plus each TLR agonist at 3 h, but neither at 6 h nor at 12 h, post-infection, was associated with induction of PspA-specific IgA and IgG in the airways. No reduction of bacterial density in the lungs of mice nasally administered PspA alone at 3 h post-infection may also be explained by a negligible level of PspA-specific IgG2a and a low level of PspA-specific IgG1 in the plasma of these mice. By contrast, no differences were found in the bacterial density in the lungs of mice nasally administered PspA plus each TLR agonist nor in mice administered PspA alone at 6 h and 12 h post-nasal challenge. These findings may be explained by the extravasation of PspA-specific IgG into the alveolar space of mice given PspA alone during the progression of lung inflammation at 6 h or 12 h post-nasal challenge [35], as a relatively low, but detectable level of PspA-specific IgG was measured in the plasma of these mice after nasal immunization. A previous study demonstrated that the induction of PspA IgG1, followed by IgG2b, but not IgG2a, by oral immunization with PspA plus cholera toxin could provide protective immunity in mice [36]. Although the opsonophagocytic activity of PspA IgG1 has not been evaluated, PspA-specific IgG1 primarily induced in plasma of mice nasally administered PspA alone should transfer from plasma to the alveolar space and act as an opsonic antibody at 6 h and 12 h post-infection. Because an influx of neutrophils occurs in the lungs within several hours after bacterial challenge in mice [37], PspA-specific IgG is likely to enhance complement fixation on the surface of bacterium [11]. Thus, opsonophagocytic killing is enhanced by accumulation of neutrophils in the lung parenchyma.

The effect of PspA plus each TLR agonist to reduce bacterial density in the nasopharynx of mice continued for 6 days after pneumococcal challenge, except for PspA plus CpG1826, in a nasopharyngeal colonization model using a serotype 19F EF3030 strain. Similar levels of PspA-specific IgG and IgA in the NW of mice nasally administered PspA plus each TLR agonist cannot explain the lack of bacterial reduction found only in mice nasally administered PspA plus CpG1826 at 6 days post-challenge. Since we previously reported the discrepancy between the level of serotype-specific IgG and opsonophagocytic functions in certain host conditions [38], the functional assays of PspA-specific IgG or IgA induced by PspA plus each TLR agonist may explain a lack of bacterial reduction found only in mice nasally administered PspA plus CpG1826 at 6 days post-infection. Further studies on the time-course of the levels of PspA-specific IgG and IgA after infection also are required.

Our data suggest that the PspA-specific antibody induced in the airway by nasal immunization with PspA plus each TLR agonist reduced the density of bacterial colonization in the upper airways of mice. A previous study also reported that intranasal immunization with PspA plus cholera toxin B subunit (CTB) induced a salivary IgA response to PspA and decreased nasopharyngeal carriage in mice [39]. However, reduction in the nasaopharyngeal carriage was greater following nasal immunization with PsaA, which is an adhesin of pneumococci, than after immunization with PspA plus CTB [5]. Another study also reported that nasal immunization with PspC, which is a paralog of PspA that is also termed CbpA, plus CTB also reduced nasopharyngeal carriage in CBA/N mice at 7 days post-bacterial challenge [40]. In an infant rat model, PspC was shown to act as a cell surface adhesin and to play a major role in nasopharyngeal colonization [41]. PspA, therefore, may also play some role in bacterial adherence in the nasopharynx of mice, although opsonophagocytic killing of *S. pneumoniae* by PspA-specific antibodies cannot be ruled out.

The complement-fixing ability of the IgG2a isotype on the bacterial surfaces is higher than other IgG isotypes [42], and PspA-specific antibodies may mediate the complement-dependent opsonophagocytic killing of *S. pneumoniae*. Therefore, Th1-associated immune responses to PspA are expected to be more efficacious for preventing pneumococcal infections, as previously reported [19,20]. However, the effects on bacterial clearance by nasal immunization with PspA plus Poly(I:C) or CpG1826, which showed a balanced IgG1/IgG2a immune response to PspA, were comparable to those by nasal immunization with PspA plus either Pam3CSK4 or LPS, which showed a predominant induction of PspA-specific IgG1 in the present study. Although the function of PspA-specific IgA remains unknown, it may play a role in bacterial clearance of the airways as PspA-specific IgG play an important role [5,20,21].

Since bacterial products, such as Pam3CSK4 and LPS, are highly toxic to humans, non-toxic TLR4 agonist, such as monophosphoryl lipid A (MPL) or *lpxL1* mutant LPS, may have clinical use as a mucosal adjuvant [13,43]. PolyI:PolyC_{12}U (Ampligen^{R}), which exhibits greatly reduced toxicity and is being used in humans, can act as a mucosal adjuvant similar to Poly(I:C) for the influenza virus [44,45]. A previous study also reported that nasal administration of CpG 1826 did not induce any local or systemic tissue damage or inflammation in mice [46]. Therefore, CpG ODN may be used as a

safe mucosal adjuvant in humans. Because the antibacterial effects of nasal immunization with PspA plus a TLR agonist were evident in the present study, the combination of a safe TLR agonist and PspA has potential clinical application as a nasal pneumococcal vaccine.

The mucosal immune system in respiratory and alimentary tracts regulates immune responses to pathogenic and commensal bacteria, and quiescently maintains the mucosal surface [47]. This review suggests the presence of a multivalent mucosa-associated regulatory system of unique mononuclear cells in the upper airways, including NALT DCs which can induce antigen-specific immune responses, although the phenotype of NALT DC has not been determined. It is conceivable that soluble TLR agonists administered with PspA may have distinct mode of distribution within the mucosa. In particular, efficiency of cellular up-take by, and the resultant activation of, the antigen presenting cells including the DCs for soluble TLR agonists may be quite different from 'endogenous' TLR agonists existing as a compartment of commensal microbes, normally restricted on mucosal surface niche. This distinct delivery mode for antigens may explain, in part, why PspA-specific antibodies were induced in the airway by nasally administered PspA plus each TLR agonist, but not by PspA alone in this study.

Pivotal but complex roles of innate immune receptors in the induction of adaptive immune responses (immunogenicity) have only recently been revealed. In fact, some innate immune receptors such as RIG-I-like receptors (RLRs) and NOD-like receptors (NLRs) have also been shown to be involved in the immunogenicity of vaccines. For example, Poly(I:C), dsRNA ligand for both TLR3 and melanoma-associated gene 5 (MDA5), works as an adjuvant mainly via MDA5, and to lesser extent, TLR3 [48]. On the other hand, although influenza A virus stimulates both TLR7 and RIG-I for innate immune activation, only the TLR7–MyD88 pathway was required for the protective adaptive immune response in mice [49]. Moreover, NLRs that sense microbial and self-derived danger particle (or crystal) molecules in the cytosol [50]. Aluminum hydroxide (alum), which is a widely used adjuvant in human vaccines, stimulates the signaling of NLR pathways for a humoral adaptive immune response [51]. Alum-mediated adjuvant activity, however, remains to be controversial [52]. Taken together, activations of TLR, RLR, or NLR on antigen presenting cells including DCs by microbial stimuli seem to have non-redundant roles in inducing the following adaptive immune responses to co-administered antigens. Presumably, Pam3CSK4 and LPS trigger activation of TLR 2 and 4 on NALT DCs, respectively. Similarly, Poly(I:C) triggers activation of both MDA5 in cytoplasm and TLR3 in endosome, and CpG 1826 activates TLR9 in endosome of NALT DCs. Therefore, nasal administration of each TLR agonist, in combination with PspA, works as potent mucosal adjuvants for induction of PspA-specific antibodies in the airways.

In conclusion, the induction of PspA-specific IgA and IgG was associated with enhanced bacterial clearance of pneumococcal strains with different serotypes from the nasopharynx and lungs of mice nasally administered PspA plus each TLR agonist. Despite the difference in the Th1- and Th2-associated IgG isotype responses among TLR agonists, bacterial clearances from the lungs at 3 h post-infection in a pneumonia model, and from nasopharynx in a colonization model at 1 day post-infection, were equivalent in mice after nasal immunization with PspA plus each TLR agonist.

Acknowledgments

We are grateful to Dr. D.E. Briles and Dr. S.K. Hollingshead from the University of Alabama at Birmingham, for providing the pneumococcal strain and the recombinant plasmid, pUAB055, for this study. This work was supported by Grants-in-Aid from the Ministry of Health, Labor and Welfare of Japan on "Mechanisms, epidemiology, prevention and control of acute respiratory infection".

References

[1] Klugman KP, Madhi SA, Huebner RE, Kohberger R, Mbelle N, Pierec N, et al. A trial of a 9-valent pneumococcal conjugate vaccine in children with and those without HIV infection. N Eng J Med 2003;349:1341–8.
[2] Cutts FT, Zaman SMA, Enwere G, Jaffar SJ, Levine OS, Okoko JB, et al. Efficacy of nine-valent pneumococcal conjugate vaccine against pneumonia and invasive pneumococcal disease in the Gambia: randomised, double-blind, placebo-controlled trial. Lancet 2005;365:1139–46.
[3] Shapiro ED, Berg AT, Austrian R, Shroeder D, Parcells V, Margolis A, et al. The protective efficacy of polyvalent pneumococcal polysaccharide vaccine. N Eng J Med 1991;325:1453–60.
[4] Briles DE, Tart RC, Swiatlo E, Dillard JP, Smith P, Benton KA, et al. Pneumococcal diversity: considerations for new vaccine strategies with emphasis on pneumococcal surface protein A (PspA). Clin Microbiol Rev 1998;11:645–57.
[5] Briles DE, Ades E, Paton JC, Sampson JS, Carlone GM, Huebner RC, et al. Intranasal immunization of mice with a mixture of the pneumococcal proteins PsaA and PspA is highly protective against nasopharyngeal carriage of *Streptococcus pneumoniae*. Infect Immun 2000;68:796–800.
[6] Ogunniyi AD, Folland RL, Briles DE, Hollingshead SK, Paton JC. Immunization of mice with combinations of pneumococcal virulence proteins elicits enhanced protection against challenge with *Streptococcus pneumoniae*. Infect Immun 2000;68:3028–33.
[7] Briles DE, Hollingshead SK, King J, Swift A, Braum PA, Park MK, et al. Immunization of human with recombinant pneumococcal surface protein A (rPspA) elicits antibodies that passively protect mice from fatal infection with *Streptococcus pneumoniae* bearing heterologous PspA. J Infect Dis 2000;182:1694–701.
[8] Nabors GS, Braun PA, Herrmann DJ, Heise ML, Pyle DJ, Gravenstein S, et al. Immunization of healthy adults with a single recombinant pneumococcal surface protein A (PspA) varient stimulates broadly cross-reactive antibodies to heterologous PspA molecules. Vaccine 2000;18:1743–54.
[9] Hollingshead SK, Becker R, Briles DE. Diversity of PspA: mosaic genes and evidence for past recombination in *Streptococcus pneumoniae*. Infect Immun 2000;68:5889–900.
[10] Tu A-H, Fulgham RL, McCrory MA, Briles DE, Szalai J. Pneumococcal surface protein A inhibits complement activation by *Streptococcus pneumoniae*. Infect Immun 1999;67:4720–4.
[11] Ren B, Szalai AJ, Hollingshead SK, Briles DE. Effects of PspA and antibodies to PspA on activation and deposition of complement on the pneumococcal surface. Infect Immun 2004;72:114–22.
[12] Holmgren J, Czerkinsky. Mucosal immunity and vaccine. Nat Med 2005;11:S45–53.
[13] Freytag LC, Clements JD. Mucosal adjuvants. Vaccine 2005;23:1804–13.
[14] Kaisho T, Akira S. Toll-like receptors as adjuvant receptors. Biochim Biophys Acta 2002;1589:1–13.
[15] Pulendran B. Modulating vaccine responses with dendritic cells and toll-like receptors. Immunol Rev 2004;199:227–50.
[16] Snapper CM, Paul WE. Interferon-γ and B cell stimulatory factor-1 reciprocally regulate Ig isotype production. Science 1987;236:944–7.
[17] Stevens TL, Bossie A, Sanders VM, Fernandez-Botran R, Coffman RL, Mosmann TR, et al. Regulation of antibody isotype secretion by subsets of antigen-specific helper T cells. Nature 1988;334:255–8.
[18] Finkelman FD, Holmes J, Katona IM, Urban Jr JF, Beckmann MP, Paul LS, et al. Lymphokine control of in vivo immunoglobulin isotype selection. Ann Rev Immunol 1990;8:303–33.
[19] Ferreira DM, Darrieux M, Oliveira MLS, Leite LCC, Miyaji EN. Optimized immune response elicited by a DNA vaccine expressing pneumococcal surface protein A is characterized by a balanced immunoglobulin G1 (IgG1)/IgG2a ration and proinflammatory cytokine production. Clin Vaccine Immunol 2008;15:499–505.
[20] Hanniffy SB, Carter AT, Hitchin E, Wells JM. Mucosal delivery of a pneumococcal vaccine using *Lactococcus lactis* affords protection against respiratory infection. J Infect Dis 2007;195:185–93.
[21] Briles DE, Hollingshead SK, Paton JC, Ades EW, Novak L, van Ginkel FW, et al. Immunization with pneumococcal surface protein A and pneumolysin are protective against pneumonia in a murine model of pulmonary infection with *Streptococcus pneumoniae*. J Infect Dis 2003;188:229–48.
[22] Briles DE, Novak L, Hotomi M, van Ginkel FW, King J. Nasal colonization with *Streptococcus pneumoniae* includes subpopulations of surfaces and invasive pneumococci. Infect Immun 2005;73:6945–51.
[23] Ozinsky A, Underhill DM, Fontenot JD, Hajjar AM, Smith KD, Wilson CB, et al. The repertoire for pattern recognition of pathogens by the innate immune system is defined by cooperation between Toll-like receptors. Proc Natl Acad Sci 2000;97:13766–71.
[24] Ichinohe T, Watanabe I, Ito S, Fujii H, Moriyama M, Tamura S, et al. Synthetic double-strand RNA Poly(I:C) combined with mucosal vaccine protects against influenza virus infection. J Virol 2005;79:2910–9.
[25] Abe N, Kodama S, Hirano T, Eto M, Suzuki M. Nasal vaccination with CpG oligodeoxynucleotide induces protective immunity against nontypeable *Haemophilus influenzae* in the nasopharynx. Laryngoscope 2006;116:407–12.
[26] Fransen F, Boog CJ, van Putten JP, van der Ley P. Agonists of toll-like receptors 3,4,7 and 9 are candidates for use as adjuvants in an outer membrane vaccine against *Neisseria meningitidis* serogroup B. Infect Immun 2007;75:5939–46.
[27] Kataoka K, McGhee JR, Kobayashi R, Fujihashi K, Shizukuishi S, Fujihashi K. Nasal Flt3 ligand cDNA elicits $CD11c^+CD8^+$ dendritic cells fro enhanced mucosal immunity. J Immunol 2004;172:3612–9.

[28] Kurita S, Koyama J, Onizuka S, Motomura K, Watanabe H, Watanabe K, et al. Dynamics of dendritic cell migration and the subsequent induction of protective immunity in the lung after repeated airway challenges by nontypeable *Haemophilus influenzae* outer membrane protein. Vaccine 2006;24:5896–903.
[29] Yoshimura A, Lien E, Ingalls RR, Toumanen E, Dziarski R, Golenbock D. Recognition of gram-positive bacterial cell wall components by the innate immune system occurs via Toll-like receptor 2. J Immunol 1999;163:1–5.
[30] Malley R, Henneke P, Morse SC, Cieslewicz MJ, Lipstich M, Thompson CM, et al. Recognition of pneumolysin by Toll-like receptors 4 confers resistance to pneumococcal infection. Proc Natl Acad Sci 2003;100:1966–71.
[31] Albiger B, Dahlberg S, Sandgren A, Wartha F, Beiter K, Katsuragi H, et al. Toll-like receptor 9 acts at an early stage in host defense against pneumococcal infection. Cell Microbiol 2007;9:633–44.
[32] Lin L, Gerth AJ, Peng SL. CpG DNA redirects class-switching towards "Th1-like" Ig isotype production via TLR 9 and Myd88. Eur J Immunol 2004;34:1483–7.
[33] Redecke V, Hacker H, Datta SK, Fermin A, Pitha PM, Broide DH, et al. Activation of Toll-like receptor 2 induces a Th2 immune response and promotes experimental asthma. J Immunol 2004;172:2739–43.
[34] Arulanandam BP, Lynch JM, Briles DE, Hollingshead S, Metzger DW. Intranasal vaccination with pneumococcal surface protein A and interleukin-12 augments antibody-mediated opsonization and protective immunity against *Streptococcus pneumoniae* infection. Infect Immun 1997;69:6718–24.
[35] Sato S, Ouellet N, Pelletier I, Shimard M, Rancourt A, Bergeron MG. Role of galectin-3 as an adhesion molecule for neutrophil extravasation during *Streptococcal pneumonia*. J Immunol 2002;168:1813–22.
[36] Yamamoto M, McDaniel LS, Kawabata K, Briles D, Jackson RJ, McGhee JR, et al. Oral immunization with PspA elicits protective humoral immunity. Infect Immun 1997:640–4.
[37] Satoh S, Oishi K, Iwagaki A, Senba M, Akaike T, Akiyama M, et al. Dexamethason impairs pulmonary defense against *Pseudomonas aeruginosa* through suppressing iNOS gene expression and peroxynitrite production in mice. Clin Exp Immunol 2002;126:266–73.
[38] Chen M, Ssali F, Mulungi M, Awio P, Yoshimine H, Kuroki R, et al. Induction of opsonophagocytic killing activity with pneumococcal conjugate vaccine in human immunodeficiency virus-infected Ugandan adults. Vaccine 2008;26:4962–8.
[39] Wu H-Y, Nham MH, Guo Y, Russel MW, Briles DE. Intranasal immunization of mice with PspA (Pneumococcal surface protein A) can prevent intranasal carriage, pulmonary infection, and sepsis with *Streptococcus pneumoniae*. J Infect Dis 1997;175:839–46.
[40] Balachandran P, Brooks-Water A, Virolainen-Julkunen A, Hollingshead S, Briles D. Role of pneumococcal surface protein C in nasopharyngeal carriage and pneumonia and its ability to elicit protection against carriage of *Streptococcus pneumoniae*. Infect Immun 2002;70:2526–34.
[41] Rosenow C, Ryan P, Weiser JN, Jhonson S, Fontan P, Ortqvist A, et al. Contribution of novel cholin-binding proteins to adherence, colonization and immunogenicity of *Streptococcus pneumoniae*. Mol Microbiol 1997;25:819–29.
[42] Oishi K, Koles NL, Guelde G, Pollack M. Antibacterial and protective properties of monoclonal antibodies reactive with *Escherichia coli* O111:B4 lipopolysaccharide: relation to antibody isotype and complement-fixing activity. J Infect Dis 1992;165:34–45.
[43] van der Ley P, Steeghts L, Mamstra HJ, ten Hove J, Zomer B, van Alphen L. Modification of lipid A biosynthesis in *Neisseria meningitides lpxL* mutants: influence on lipopolysaccharide structure, toxicity, and adjuvant activity. Infect Immun 2001;69:5981–90.
[44] Thompson KA, Strayer DR, Salvato PD, Thompson CE, Klimas N, Molavi A, et al. Results of a double-blind placebo-controlled study of the double-stranded RNA drug Polyl:PolyC_{12}U in the treatment of HIV infection. Eur J Clin Microbiol Infect Dis 1996;15:580–7.
[45] Ichinohe T, Tamura S, Kawaguchi A, Ninomiya A, Imai M, Itamura S, et al. Cross-protection against H5N1 influenza virus infections is afforded by intranasal inoculation with seasonal trivalent inactivated influenza vaccine. J Infect Dis 2007;196:1313–20.
[46] Kodama S, Abe N, Hirano T, Suzuki M. Safety and efficacy of nasal application of CpG oligodeoxynucleotide as a mucosal adjuvant. Laryngoscope 2006;116:331–5.
[47] Kunisawa J, Nochi T, Kiyono H. Immunological commensalities and distinctions between airway and digestive immunity. Trends Immunol 2008;29:505–13.
[48] Kumar H, Koyama S, Ishii KJ, Kawai T, Akira S. Cutting edge: cooperation of IPS-1- and TRIF-dependent pathways in poly IC-enhanced antibody production and cytotoxic T cell responses. J Immunol 2008;180:683–7.
[49] Koyama S, Ishii K, Kumar H, Tanimoto T, Coban C, Uematsu S, et al. Differential role of TLR- and RLR-signaling in the immune responses to influenza A virus infection and vaccination. J Immunol 2007;179:4711–20.
[50] Mariathosan S, Monack DM. Inflammasome adaptors and sensors: intracellular regulators of infection and inflammation. Nat Immunol Rev 2007;7:31–40.
[51] Eisenbarth SC, Colegio OR, O'Connor Jr W, Sutterwala FS, Flavell RA. Crucial role for the Nalp3 inflammasome in the immunostimulatory properties of aluminium adjuvants. Nature 2008;453:1122–6.
[52] Franchi L, Nunez G. The Nlrp3 inflammasome is critical for aluminum hydroxide-mediated IL-1 β secretion but dispensable for adjuvant activity. Eur J Immunol 2008;38:2085–9.

総　説

劇症型溶血性レンサ球菌感染症の発症機序
—菌の免疫回避機構と菌の特性—

[1]国立感染症研究所・細菌第一部，[2]同　免疫部
池辺　忠義[1]　阿戸　学[2]　小林　和夫[2]　渡辺　治雄[1]

(平成20年12月26日受付)
(平成21年7月7日受理)

Key words: streptococcal toxic shock-like syndrome, neutrophil, interleukin-8, streptolysin O, serine protease

要　旨

劇症型溶血性レンサ球菌感染症（streptococcal toxic shock syndrome）は，1987年に米国で最初に報告され，日本においても1992年に典型的な症例が報告されている．現在までに500人を超える患者が確認され，このうち約40%が死亡しているというきわめて致死率の高い感染症である．病理学的所見から，感染部位において菌の集積はあるが，多核白血球の浸潤が見られないことから，宿主防御の撹乱が劇症型溶血性レンサ球菌感染症の発症機序に重要であることが考えられた．そこで多核白血球に対する作用を調べた結果，劇症型感染症を引き起こした株は，少なくとも2つの方法によって，多核白血球の機能を阻害していることが判明した．1つは，ストレプトリジンOによる多核白血球のネクローシス，もう1つは，セリンプロテアーゼであるScpCによりIL-8を切断することで多核白血球の遊走能を阻害することである．これらの因子をコードする遺伝子の発現は，劇症型感染症を引き起こした株で増大しており，この発現の上昇は，二成分制御系の*csrS*遺伝子の変異によるものであった．

〔感染症誌　83：485～489，2009〕

はじめに

劇症型溶血性レンサ球菌感染症（streptococcal toxic shock syndrome）は，1987年に米国で最初に報告され[1)2)]，その後，先進国ばかりでなく発展途上国からも報告されている再興感染症の一つである．日本における最初の典型的な症例は1992年に報告されており[3)]，現在までに500人を超える患者が確認されている．そして，このうち約40%が死亡しているというきわめて致死率の高い感染症である．この感染症の主な病原菌は，A群レンサ球菌（*Streptococcus pyogenes*）であり，古くから咽頭炎，扁頭炎，猩紅熱，続発症としてリウマチ熱や急性糸球体腎炎などを引き起こすことで知られている．本総説では，劇症型溶血性レンサ球菌感染症由来株と非劇症株との違いについて免疫回避，菌の特性について現在までの知見をまとめた．

劇症型溶レン菌感染症患者分離株の疫学および病態

劇症型溶血性レンサ球菌感染症は，初期症状として，四肢の疼痛，腫脹，発熱，血圧低下などがみられ，発病から病態の進行が急激かつ劇的で，いったん発病すると数十時間以内に急性腎不全，成人型呼吸窮迫症候群（ARDS），播種性血管内凝固症候群（DIC），多臓器不全（MOF），軟部組織壊死を引き起こし，患者をショック症状から死に至らしめる．

1999年4月に施行された「感染症の予防及び感染症の患者に対する医療に関する法律（感染症法）」による集計によると，2000年には45例，2001年には43例，2002年には90例，2003年には52例，2004年には53例，2005年には60例が報告されている．2006年の感染症法の改正で，劇症型溶血性レンサ球菌感染症の届出基準が一部変更され，それまでA群レンサ球菌に限定していたが，この改正でβ溶血を示すレンサ球菌にまで広げられた．感染症法に基づく医師及び獣医師の届出は厚生労働省のホームページに記載されている（http://www.mhlw.go.jp/bunya/kenkou/kekkaku-kansenshou11/01-05-06.html）．改正後，年間約100例が報告されている（2006年107例，2007年

別刷請求先：（〒162-8640）東京都新宿区戸山1—23—1
国立感染症研究所細菌第一部　池辺　忠義

平成21年9月20日

図　Invasive GAS strain evasion mechanisms

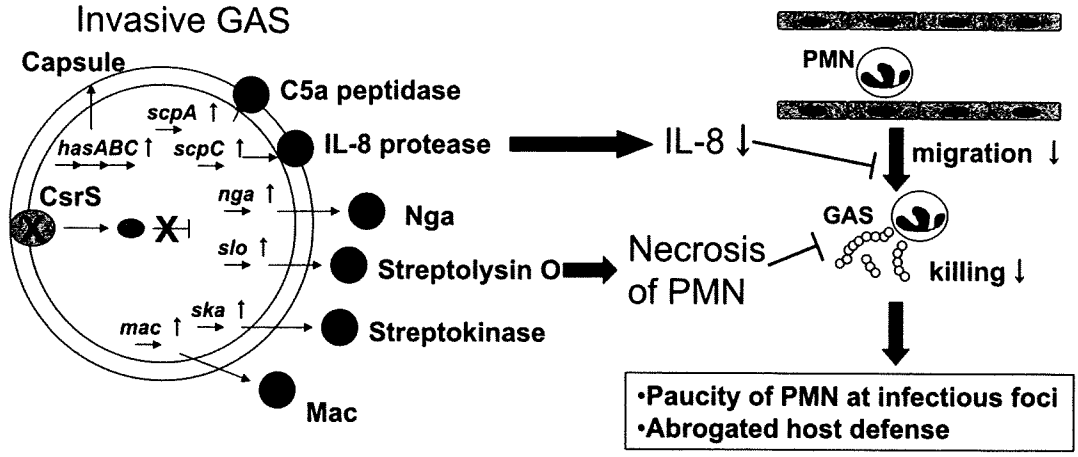

GAS: group A streptococcus, PMN: polymorphoneutrophil, IL-8: Interleukin-8

2000年になってから，1999年以前にみられなかった型の菌が分離されてきている[12]．国立感染症研究所細菌第一部に集められたA群レンサ球菌による劇症型/重症溶レン菌感染症患者分離株の*emm*型は，31種類にも及んでいる．

A群レンサ球菌の主な病原性因子

A群レンサ球菌の病原性因子は，他の細菌と比べ非常に多彩であるとともに，A群レンサ菌の中でも保有している病原性因子が菌株により異なる．細胞障害に関与するものとして，ストレプトリジンO(SLO)やストレプトリジンS (SLS)，NADアーゼ (Nga) などが知られている．ストレプトキナーゼ (Ska) は，線溶系を活性化し，血液凝固を阻止する因子である．タンパク分解酵素の中には，システインプロテアーゼであるSpeB，補体であるC5aやC3を分解するC5aペプチダーゼ (ScpA)，C3プロテアーゼ，IL-8分解酵素であるScpC/SpyCEPなどがある．この他，抗体を分解するEndoSやMac/IdeSなどが知られている．Sicタンパク質は，補体阻害因子として機能する．さらに，T細胞活性化因子として，SpeA，SpeC，SpeG，SpeH，SpeI，SpeJ，SpeK，SpeL，SpeM，SSAなどのスーパー抗原も知られている．接着因子として，フィブロネクチン結合タンパク質 (PrtF1/SfbI，Pfbp，SfbII，FbaB，SfbX)，ラミニン結合タンパク質(Lbp)，ヒアルロン酸莢膜，Mタンパクなどが知られおり，これらは，粘膜上皮，ケラチノサイトや細胞外マトリクスなどに接着するときに重要な役割を示すことが知られている．

劇症型溶血性レンサ球菌感染症患者由来株に関する知見

劇症型溶血性レンサ球菌感染症の病理像の特徴の一つとして，病巣に菌の集積が見えるにもかかわらず，溶血性レンサ球菌による感染を最前線で防御する多核白血球の遊走がみられないことが報告されている[13]．このことは，宿主防御因子，特に多核白血球の病巣における欠如が劇症型溶血性レンサ球菌感染症に重要な役割をもっていることが示唆される．我々は，2000年以降分離され始めた*emm49*型の劇症型/重症溶血性レンサ球菌感染症患者分離株と非劇症型感染症患者分離株を用いて，IL-8添加時の好中球の遊走能および殺菌能の違いについて解析した．その結果，劇症型溶血性レンサ球菌感染症患者分離株は，非劇症型患者分離株と比較して，好中球の遊走能を低下させ，また，たとえ遊走したとしても，遊走した好中球のほとんどを死滅させることが判明した[14]．この原因として，劇症型溶血性レンサ球菌感染症でみられる多核白血球の病巣における欠如は，少なくとも2段階の作用によって行われていることが明らかとなった．1つ目は，好中球の遊走性の阻止である．これはA群レンサ球菌がもつセリンプロテアーゼであるScpC/SpyCEPタンパク質が，好中球の遊走因子であるIL-8を分解し，好中球の遊走を阻害することによるものである．2つ目は，好中球のネクローシスである．これは，A群レンサ球菌が分泌する細胞障害因子であるストレプトリジンO (SLO) タンパク質が好中球をネクローシスさせることによるものである[14]．

非劇症株と劇症型患者分離株とでは，*scpC*および*slo*遺伝子の配列に違いが見られないことから，構造遺伝子の変異ではないことが考えられた．そこで，RT-PCRによりScpC/SpyCEPタンパク質やストレプトリジンOをコードする遺伝子の発現量を調べたところ，劇症型溶血性レンサ球菌感染症患者分離株のほう

平成21年9月20日

表

衛生微生物協議会溶血性レンサ球菌レファレンスシステムセンター窓口

A群レンサ球菌のT, M型別試験, および劇症型A群レンサ球菌感染症に関する情報についての窓口は以下の機関になっておりますので, お問い合わせをお願いいたします.

センター
国立感染症研究所 細菌第一部 〒162-8640 東京都新宿区戸山1—23—1
tel：03-5285-1111 fax：03-5285-1163
北海道・東北・新潟ブロック支部センター
福島県衛生研究所 微生物課 〒960-8163 福島県福島市方木田字水戸内16—6
tel：024-546-8047 fax：024-546-8364
関東・甲信越静ブロック支部センター
神奈川県衛生研究所 微生物部 〒253-0087 神奈川県茅ヶ崎市下町屋1—3—1
tel：046-783-4400 fax：046-783-4457
東京都支部センター
東京都健康安全研究センター 微生物部 〒169-0073 東京都新宿区百人町3—24—1
tel：03-3363-3231 fax：03-3368-4060
東海・北陸ブロック支部センター
富山県衛生研究所 細菌部 〒939-0363 富山県射水市中太閤山17—1
tel：0766-56-8142 fax：0766-56-7326
近畿ブロック支部センター
大阪府立公衆衛生研究所 感染症部 〒537-0025 大阪府大阪市東成区中道1—3—69
tel：06-6972-1321 fax：06-6972-0772
中国・四国ブロック支部センター
山口県環境保健センター 保健科学部 〒753-0821 山口県山口市葵2—5—67
tel：083-922-7630 fax：083-922-7632
九州ブロック支部センター
大分県衛生環境研究センター 微生物担当 〒870-1117 大分県大分市高江西2—8
tel：097-554-8984 fax：097-554-8987

96例, 2008年111例).

Stevensら[4)5)]の報告によると, 劇症型溶血性レンサ球菌感染症のもっとも一般的な初期症状として, 四肢の疼痛が急激に始まり, その部位で圧痛が認められた. 疼痛は, 多くの場合, 四肢で見られ, 疼痛の開始前に, 約20%の患者で, 発熱, 悪寒, 筋肉痛, 下痢のようなインフルエンザ様の症状を示す場合があった. 臨床所見として, 発熱が, 最も一般的な徴候である（ただし, 患者の10%では発見時にすでにショックによる低体温を示す例がある). 錯乱状態（confusion）は患者の55%で見られ, 患者によっては, 昏睡や好戦的な姿勢を示すことがある. 局所的な腫脹, 圧痛, 疼痛, 紅斑のような軟部組織感染の徴候は, 皮膚の傷口が存在する場合によく見られた. 発熱を持つ患者で紫色の水疱が圧痛のある部位にみられると, 筋炎や壊死性筋膜炎のような深部の軟部組織感染を起こしている可能性が考えられた[6)]. Stevenら[4)]の報告によると, 劇症型溶血性レンサ球菌感染症の患者の約35%は皮膚(minor trauma, surgical procedures, intravenous drug abuse), あるいは, 約20%は粘膜(pharynx, vagina)からの*S. pyogenes*の感染であり, 残りの約45%は, 正確な菌の侵入部位が不明であった.

劇症型/重症溶レン菌感染症患者由来株の分子疫学

A群レンサ球菌には, TタンパクやMタンパク, Rタンパクなど数多くの表層抗原因子が知られている. このうちMタンパクは, 型特異的であり, 100以上の型が知られていることから[7)], 菌の疫学マーカーとしてよく用いられている. Mタンパクは, 抗オプソニン作用[8)9)]を有し, 細胞への接着にも関与しており, 病原因子として知られている. 分離株のM型別を行うことは病因との関連を知る上で重要である. 近年, M型別を血清学的方法ではなく, Mタンパクをコードする遺伝子（*emm*）の塩基配列を決定することで, 遺伝子による型別が可能となった. この*emm*遺伝子は, A群以外に, C群やG群レンサ球菌も保有しており, C, G群レンサ球菌の型別にも利用可能となった. これらのデータベースはCDCのホームページに記載されている（http://www.cdc.gov/ncidod/biotech/strep/strepindex.htm).

2008年11月30日までに衛生微生物技術協議会溶血性レンサ球菌レファレンスシステムセンター（表）に集められたA群レンサ球菌による劇症型/重症溶レン菌感染症患者分離株に395株ついて, *emm*遺伝子型を調べたところ, 最も多い型は, *emm1*型で, 44.3%（175株）を占める. 続いて*emm3*型（11.6%, 46株), *emm28*型（7.6%, 30株), *emm12*型（6.6%, 26株）である. 劇症型溶血性レンサ球菌感染症患者から分離される*S. pyogenes*の*emm*型は, 1992～1995年までは, *emm3*型と*emm1*型が主であったが, 1995年以降, *emm3*型は減少し, *emm1*型が主流となっている[10)11)]. また,

が，非劇症株より，発現量の増大が確認された．このことから，劇症型溶血性レンサ球菌感染症患者分離株は，IL-8プロテアーゼやストレプトリジンO遺伝子の発現量を増大させ，好中球の機能障害を起こしていることが判明した[14]．

IL-8プロテアーゼやストレプトリジンOをコードする遺伝子の発現の増大が何に起因しているのかを調べたところ，劇症型溶血性レンサ球菌感染症患者分離株において，CsrS/CovSという二成分制御因子のセンサータンパク質に変異があることが判明した．このタンパク質は，環境の変化に応じてシグナルを負の転写制御因子に伝えるセンサータンパク質である．転写制御因子により発現が抑えられていた遺伝子群（IL-8プロテアーゼやストレプトリジンOをコードする遺伝子を含む）は，*csrS* 遺伝子に変異が生じることにより，脱抑制され，IL-8プロテアーゼやストレプトリジンO等をコードする遺伝子の発現量を増大させていることが明らかになった（図）[14]．

おわりに

劇症型溶血性レンサ球菌感染症は，病態の進行が急激かつ劇的で，患者をショック症状から死に至らしめる．我々の研究の結果から，多核白血球からの殺菌逃避機序として2つの病原因子の関与が明らかとなった．これら2つの因子は，劇症型溶血性レンサ球菌感染症患者分離株において発現が上昇していた．この発現の上昇は，負の制御因子であるCsrSの変異による遺伝子発現の脱抑制によるものである．この制御因子は，様々な遺伝子の発現を負に制御していることから，この遺伝子の変異により，様々な病原性遺伝子の発現が増大しているものと考えられる．したがって，この制御下にある今回見い出した2つの病原因子以外の病原因子をさらに解析することにより，劇症型溶血性レンサ球菌感染症の全体像が明らかになることが期待される．

文　献

1) Weiss KA, Laverdiere M : Group A Streptococcus invasive infections ; A review. Can J Surg 1997 ; 40 : 18—25.
2) Stevens DL : The flesh-eating bacterium : what's next? J Infect Dis 1999 ; 179 (Suppl 2) : S366—74.
3) Shimizu Y, Ohyama A, Kasama K, Miyazaki M, Ooe K, Ookochi Y : Case report of toxic shock-like syndrome due to group A streptococcal infection. Kansenshogaku Zasshi 1993 ; 67 : 236—9.
4) Stevens DL, Tanner MH, Winship J, Swarts R, Ries KM, Schlievert PM, *et al.* : Severe group A streptococcal infections associated with a toxic shock-like syndrome and scarlet fever toxin A. N Engl J Med 1989 ; 321 : 1—7.
5) Stevens DL : Invasive group A streptococcus infections. Clin Infect Dis 1992 ; 14 : 2—13.
6) Stevens DL : Streptococcal infections of skin and soft tissue. In : Stevens DL, Mandell GL, eds. In Atlas of Infectious Diseases. Churchill Livingstone, New York, 1995 ; p. 3.1—3.11.
7) Centers for Disease Control and Prevention Homepage. *Streptococcus pyogenes* database. http://www.cdc.gov/ncidod/biotech/strep/strepindex.html.
8) Horstmann RD, Sievertsen HJ, Knobloch J, Fischetti VA : Antiphagocytic activity of streptococcal M protein : selective binding of complement control protein factor H. Proc Natl Acad Sci USA 1988 ; 85 : 1657—61.
9) Fischetti VA : Streptococcal M protein : molecular design and biological behavior. Clin Microbiol Rev 1989 ; 2 : 285—300.
10) Inagaki Y, Konda T, Murayama S, Yamai S, Matsushima A, Gyobu Y, *et al.* : Serotyping of *Streptococcus pyogenes* isolated from common and severe invasive infections in Japan, 1990-5 : implication of the T3 serotype strain-expansion in TSLS. Epidemiol Infect 1997 ; 119 : 41—8.
11) Ikebe T, Murai N, Endo M, Okuno R, Murayama S, Saitoh K, *et al.* : Changing prevalent T serotypes and *emm* genotypes of *Streptococcus pyogenes* isolates from streptococcal toxic shock-like syndrome (TSLS) patients in Japan. Epidemiol Infect 2003 ; 130 : 569—72.
12) Ikebe T, Hirasawa K, Suzuki R, Ohya H, Isobe J, Tanaka D, *et al.* : Distribution of *emm* genotypes among group A streptococcus isolates from patients with severe invasive streptococcal infections in Japan, 2001-2005. Epidemiol. Infect 2007 ; 135 : 1227—9.
13) Hidalgo-Grass C, Dan-Goor M, Maly A, Eran Y, Kwinn LA, Nizet V, *et al.* : Effect of a bacterial pheromone peptide on host chemokine degradation in group A streptococcal necrotising soft-tissue infections. Lancet 2004 ; 363 : 696—703.
14) Ato M, Ikebe T, Kawabata H, Takemori T, Watanabe H : Incompetence of neutrophils to invasive group A *streptococcus* is attributed to induction of plural virulence factors by dysfunction of a regulator. PLoS ONE 2008 ; 3 : e3455.

Mechanism Behind Streptococcus Toxic Shock-like Syndrome Onset —Immune Evasion and Bacterial Properties—

Tadayoshi IKEBE[1], Manabu ATO[2], Kazuo KOBAYASHI[2] & Haruo WATANABE[1]
[1]Department of Bacteriology and [2]Department of Immunology, National Institute of Infectious Diseases

Streptococcal toxic shock-like syndrome (STSS) was firstly reported in 1987 in the United States. Japan's first definitive STSS case was reported in 1992, with over 500 cases since confirmed. Mortality is extremely high at 40%. Pathological findings, bacteria aggregation, and a paucity of polymorphonuclear neutrophils (PMN) in the foci of invasive group A streptococcal (GAS) infection suggest that host defense disturbance plays an important role in invasive infection onset. GAS, clinically isolated from severely invasive, but not from non-invasive, infections, could compromise human PMN functions in at least two independent ways-by inducing necrosis to PMN by enhanced production of pore-forming toxin streptolysin O (SLO) and by PMN migration impairment via digesting interleukin-8, a PMN attracting chemokine, through increased serine protease ScpC production. Expression of these genes was upregulated by a loss of repressive function with the *csrS* gene mutation of the two-component sensor/regulator system.

平成21年9月20日

INFECTION AND IMMUNITY, Nov. 2009, p. 4806–4814 Vol. 77, No. 11
0019-9567/09/$12.00 doi:10.1128/IAI.00577-09

CD46 Transgenic Mouse Model of Necrotizing Fasciitis Caused by *Streptococcus pyogenes* Infection▽

Hidenori Matsui,[1]†* Yukie Sekiya,[1]† Masahiko Nakamura,[2]* Somay Yamagata Murayama,[1] Haruno Yoshida,[1] Tetsufumi Takahashi,[2] Ken'ichi Imanishi,[3] Kanji Tsuchimoto,[2] Takehiko Uchiyama,[3,4] Keisuke Sunakawa,[1] and Kimiko Ubukata[1]

Kitasato Institute for Life Sciences and Graduate School of Infection Control Sciences, Kitasato University, 5-9-1 Shirokane, Minato-ku, Tokyo 108-8641, Japan[1]; Center for Clinical Pharmacy and Clinical Sciences, School of Pharmaceutical Sciences, Kitasato University, 5-9-1 Shirokane, Minato-ku, Tokyo 108-8641, Japan[2]; Department of Microbiology and Immunology, Tokyo Women's Medical University School of Medicine, 8-1 Kawada-cho, Shinjuku-ku, Tokyo 162-8666, Japan[3]; and College of Human Science, Tokiwa University, 1-430-1 Miwa, Mito-shi, Ibaraki 310-8585, Japan[4]

Received 23 May 2009/Returned for modification 9 July 2009/Accepted 26 August 2009

We developed a human CD46-expressing transgenic (Tg) mouse model of subcutaneous (s.c.) infection into both hind footpads with clinically isolated 11 group A streptococcus (GAS) serotype M1 strains. When the severity levels of foot lesions at 72 h and the mortality rates by 336 h were compared after s.c. infection with 1×10^7 CFU of each GAS strain, the GAS472 strain, isolated from the blood of a patient suffering from streptococcal toxic shock syndrome (STSS), induced the highest severity levels and mortality rates. GAS472 led to a 100% mortality rate in CD46 Tg mice after only 168 h postinfection through the supervention of severe necrotizing fasciitis (NF) of the feet. In contrast, GAS472 led to a 10% mortality rate in non-Tg mice through the supervention of partial necrotizing cutaneous lesions of the feet. The footpad skin sections of CD46 Tg mice showed hemorrhaging and necrotic striated muscle layers in the dermis, along with the exfoliation of epidermis with intracellular edema until 48 h after s.c. infection with GAS472. Thereafter, the bacteria proliferated, reaching a 90-fold or 7-fold increase in the livers of CD46 Tg mice or non-Tg mice, respectively, for 24 h between 48 and 72 h after s.c. infection with GAS472. As a result, the infected CD46 Tg mice appeared to suffer severe liver injuries. These findings suggest that human CD46 enhanced the progression of NF in the feet and the exponential growth of bacteria in deep tissues, leading to death.

Group A streptococci (GAS), which are among the most common human pathogens, can cause a variety of uncomplicated superficial skin infections such as impetigo/pyoderma or throat infections, including streptococcal pharyngitis (sore throat) and tonsillitis (3). In addition, patients suffering from acute and complicated GAS infections, in particular streptococcal toxic shock syndrome (STSS) associated with severe necrotizing fasciitis (NF), have high mortality rates (4). M proteins, which attach to the cell wall, are one of the important virulence factors that GAS possess (15). The various GAS strains have more than 100 different antigenically distinguishable M proteins (46), and GAS serotype M1 strains are regarded as a highly virulent group (3).

Membrane cofactor protein (MCP; CD46), which is expressed in every cell type except erythrocytes, is implicated as a receptor for at least six human pathogens (four viruses and two bacteria), including measles virus (9, 31, 35), herpesvirus 6 (40), adenovirus groups B (17, 41) and D (48), pathogenic *Neisseria* (23), and GAS (37). Human CD46-expressing transgenic (Tg) mice are susceptible to streptococcal disease (30). When CD46 Tg and non-Tg mice were infected intravenously (i.v.) with GAS, the bacteremia levels, frequency of arthritis, and mortality rate were higher in CD46 Tg mice than in non-Tg mice (30). Unfortunately, this animal model does not reflect the natural infection process in the human host. Consequently, we have attempted to establish a CD46 Tg mouse model of skin and soft tissue infection with GAS that closely represents the human disease. If the disease pathogenesis in an animal model is in many ways very similar to that observed in humans, it will enable researchers to address a variety of questions regarding the development of urgently needed diagnostic methods and therapies. To the best of our knowledge, this is the first report to create the CD46 Tg mouse model of subcutaneous (s.c.) infection with GAS472 (a serotype M1 strain isolated from the blood of a patient suffering from STSS) into both hind footpads, thereby causing an acute disease that mimics severe NF in human.

MATERIALS AND METHODS

Bacterial strains and culture conditions. Beta-hemolytic GAS serotype M1 strains collected in Japan in 2006 are described in Table 1. GAS strains were preserved in 10% (wt/vol) skim milk and stored at −85°C until use. The frozen GAS strains were streaked onto sheep blood agar plates (Nippon Becton Dickinson, Tokyo, Japan) and cultured overnight at 37°C in a humidified 5% CO_2 incubator. Prior to their use in infection experiments, GAS strains were grown on Todd-Hewitt broth containing 0.2% (wt/vol) yeast extract (THY; Difco and BBL, Detroit, MI) in 5% CO_2 at 37°C without shaking.

* Corresponding author. Mailing address: Kitasato Institute for Life Sciences and Graduate School of Infection Control Sciences, Kitasato University, 5-9-1 Shirokane, Minato-ku, Tokyo 108-8641, Japan. Phone and fax for H. Matsui: 81-3-5791-6267. E-mail: hmatsui@lisci.kitasato-u.ac.jp. Phone and fax for M. Nakamura: 81-3-3446-9036. E-mail: nakamuram@pharm.kitasato-u.ac.jp.
† H.M. and Y.S. contributed equally.
▽ Published ahead of print on 8 September 2009.

TABLE 1. Characteristics of 11 clinical isolates of GAS serotype M1

GAS strain	Patient age (yr)	Patient sex	Diagnosis	Collection source	Patient survival status
GAS472	38	Male	STSS	Blood	Dead
GAS467	57	Male	Meningitis, sepsis	CSF[a]	Dead
RE335	6	Female	Pyogenic arthritis	Blood	Alive
RE025	76	Male	NF	Tissue specimens	Dead
GAS465	7	Female	Pharyngitis	Pharyngeal swab	Alive
RE386	62	Female	Pharyngitis, sinusitis	Blood	Alive
RE137	72	Male	Meningitis	CSF	Dead
RE303	52	Male	Sepsis[b]	SCA[c]	Dead
RE157	75	Male	Facial cellulitis	Blood	Alive
GAS453	9	Male	PCA[d]	Pharyngeal swab	Alive
RE344	40	Female	Sepsis[e]	Blood	Alive

[a] CSF, cerebrospinal fluid.
[b] Chronic renal failure (preexisting disease).
[c] SCA, subendocardial abscess.
[d] PCA, pyogenic cervical adenitis.
[e] Acute hepatitis (preexisting disease).

Mouse model for GAS infection. The human CD46-expressing Tg mice were a generous gift from J. P. Atkinson, Washington University. CD46 Tg mice possess two copies of human CD46 gene per diploid genome, and the expression levels of CD46 RNA and protein were comparable to those observed in matched human tissues, including muscle, fat, and skin (25). Using immunohistochemistry, human CD46 was found on epithelial cells, endothelial cells, glial cells, and hepatocytes; in the glomerulus (in kidney) and adrenal gland; as well as on B cells, T cells, neutrophils, and macrophages (22). The CD46 Tg mice used in this study had the C57BL/6 genetic background (*H-2*^{b} haplotype). In previous studies, C57BL/6 (21, 22, 25, 34) or B6C3F1 (*H-2*^{bk}) (30, 42) mice have been used as non-Tg control mice. Therefore, to begin this study, we used both C57BL/6 and B6C3F1 mice obtained from Charles River Japan (Yokohama, Japan) as non-Tg control mice. The expression of many pathogenic traits of GAS has been shown to depend on the growth phase (33). Thus, 7-week-old mice were s.c. infected with a total of 1×10^7 CFU of stationary-growth-phase GAS into both hind footpads (5×10^6 CFU per footpad). After s.c. infection, the survival rates were observed every 24 h for 336 h postinfection, or the number of bacteria in the blood and tissue samples including the popliteal lymph nodes (PLN), spleen, and liver were determined by plating onto sheep blood agar (11, 27). All mice were bred at the animal facility at the Kitasato Institute, and all mouse experiments were performed in accordance with institutional protocol guidelines under an approved protocol.

Macroscopic and microscopic observations. Macroscopic images were obtained with a digital camera (D80; Nikon, Tokyo, Japan). For histological examination, a portion of each footpad and a portion of each liver were fixed with 10% (vol/vol) buffered formalin and then embedded in paraffin. Tissue sections approximately 5 μm thick were prepared and mounted on glass slides. The slides were stained with hematoxylin and eosin (H&E) and Giemsa. Alternatively, another portion of each liver was also fixed with Zamboni's fixative (2% [wt/vol] paraformaldehyde and 15% [vol/vol] saturated picric acid in 0.1 M phosphate buffer, pH 7.3) for at least 8 h at 4°C (44), and the 4-μm cryostat sections obtained were stained with Alexa Fluor 594-conjugated phalloidin (Molecular Probes, Eugene, OR) at a dilution of 1:1,000. The sections were mounted in Permafluor and were observed by confocal laser microscopy (TCS NT; Leica Biosystems, Nussloch, Germany).

Transcription analysis. The bacterial cells of GAS472 grown in THY broth were washed once with Dulbecco's modified Eagle's medium (Sigma-Aldrich, St. Louis, MO) and suspended in Dulbecco's modified Eagle's medium. The bacterial cell suspension (1×10^8 CFU) was mixed with an equal volume of whole blood from CD46 Tg or C57BL/6 mice collected by cardiac puncture with a heparin-coated 23-gauge needle. The mixture was then placed in a 37°C humidified 5% CO_2 incubator. At 0, 1, 2, and 6 h of incubation, bacterial cells were harvested by centrifugation and washed three times with cold distilled water. Gene expression patterns of GAS472 were determined by quantitative real-time reverse transcription (RT)-PCR analysis. Total RNA extracted from bacterial cells using the RNeasy Protect bacteria minikit with on-column RNase-free DNase I treatment (Qiagen Sciences, Germantown, MD) was subjected to the RT reaction from 100 ng of total RNA in a 20-μl reaction volume using the iScript cDNA synthesis kit (Bio-Rad Laboratories, Hercules, CA). The following real-time PCR assays were performed with RNA templates to ensure that contaminating genomic DNA was absent before the RT reaction. Quantitative real-time PCR in triplicate on 1 μl of template cDNA per 10-μl reaction was performed in a CFX96 real-time PCR detection system (Bio-Rad Laboratories) using the iQ SYBR green supermix (Bio-Rad Laboratories). Gene-specific primer pairs (16S rRNA, 5′-GAGAGACTAACGCATGTTAGTA-3′ and 5′-TAGTTACCGTCACTTGGTGG-3′; *sagA*, 5′-TGCTGCTGCTGCTGTACTAC-3′ and 5′-GCTTCCGCTACCACCTTGAG-3′) were designed using Beacon Designer 7.5. The PCR conditions included an initial denaturation step at 95°C for 3 min, followed by 50 amplification cycles of denaturation at 95°C for 10 s, annealing at 52°C for 10 s, and extension at 72°C for 30 s.

Genotypic analysis of GAS. For a comparison of the DNA sequences of the *csrRS* (also called *covRS*) locus between virulent (GAS472 and GAS467) and avirulent (RE386 and RE344) strains of GAS, we used 12 primers (p1 to p12) as previously described by Walker et al. (47). We used an ABI 3130 automatic sequencer (Applied Biosystems, Foster City, CA) for the direct sequence of the amplified PCR products (3,018 bp) with the primer pair p1/p12. The determined DNA sequences were assembled by the use of a component of Vector NTI version10.3.1 (Invitrogen, Carlsbad, CA).

Statistics. Significant differences between the means ± standard deviations (SDs) of different groups were examined using a two-tailed unpaired Student's *t* test (see Fig. 6) or a one-tailed paired Student's *t* test (see Fig. 8). A P value of <0.05 was regarded as statistically significant.

RESULTS

CD46 Tg mice exhibited necrotizing lesions of the feet 72 h after s.c. infection with GAS strains. As shown in Fig. 1, we classified 11 GAS strains into two groups associated with the severity levels of foot lesions in CD46 Tg mice 72 h after infection with GAS strains. In the first group, the feet developed well-defined necrosis (GAS472, GAS467, and RE025). The second group showed swelled feet (the skin appeared red and blotchy) and occasionally blisters (RE335, GAS465, GAS453, RE303, RE386, RE137, RE157, and RE344). All infected CD46 Tg mice were still alive in this time period. In contrast, even in the worst cases, the necrotizing cutaneous lesions developed partially in the feet of non-Tg mice 72 h after infection with GAS472 (Fig. 2A and B). Alternatively, the feet merely swelled up or developed minor wounds in non-Tg mice 72 h after infection with GAS467 (Fig. 2C and D) or RE335 (Fig. 2E and F). These results demonstrate that GAS472 had the strongest virulence traits among the 11 GAS strains essential for causing necrotizing lesions. Accordingly, we selected and used GAS472 for the following histological study.

The footpad skin sections of CD46 Tg and non-Tg mice

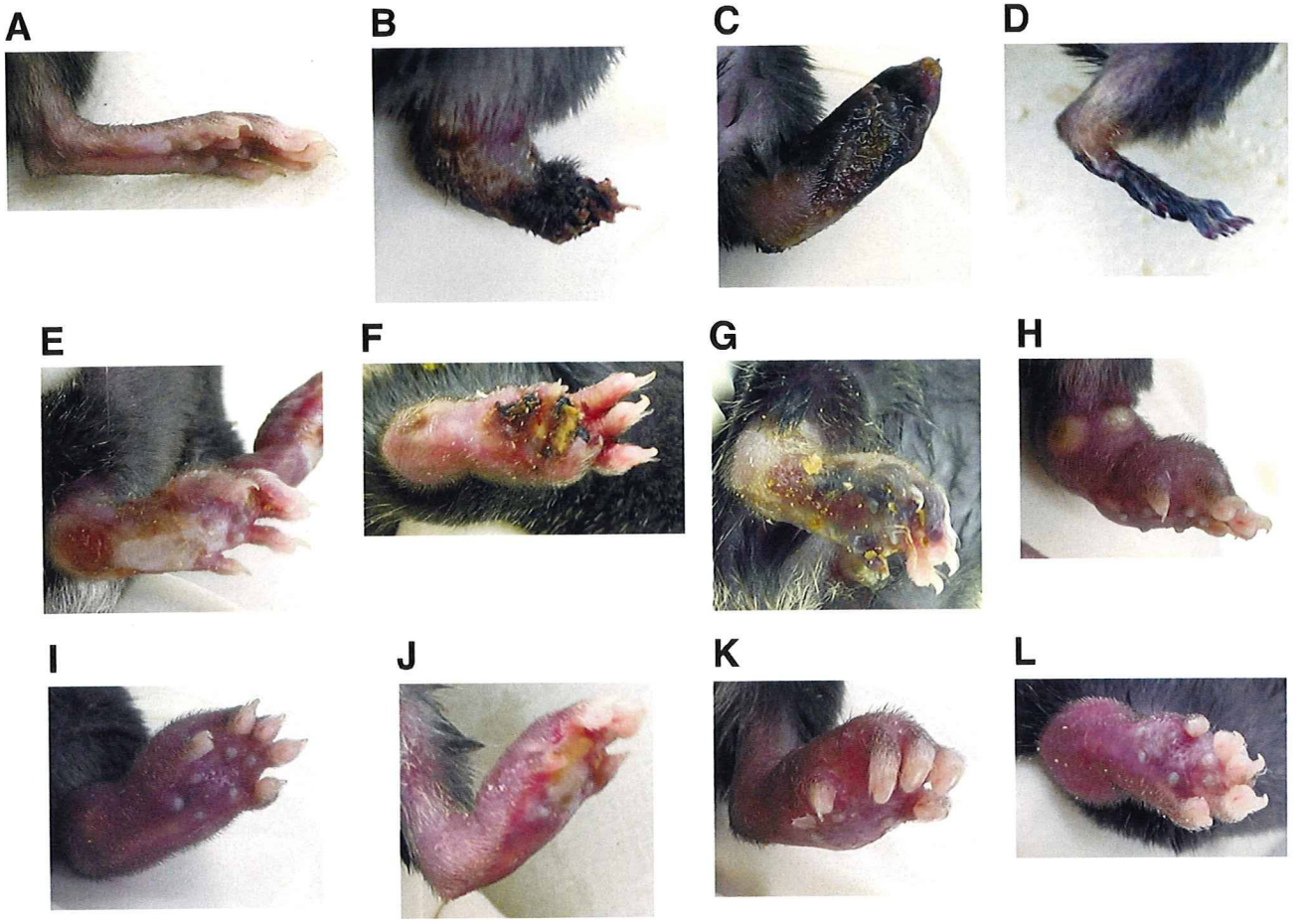

FIG. 1. Representative appearance of necrotizing lesions of CD46 Tg mouse feet. Shown is the macroscopic observation of CD46 Tg mouse foot 72 h after s.c. infection with 5×10^6 CFU of the GAS strains GAS472 (B), GAS467 (C), RE025 (D), RE335 (E), GAS465 (F), GAS453 (G), RE303 (H), RE386 (I), RE137 (J), RE157 (K), and RE344 (L) per footpad. Panel A shows noninfection.

exhibited acute inflammation (neutrophil infiltration) in the hypodermis 6 h after infection with GAS472. At 24 h postinfection, although increased inflammatory cell infiltration was recognized in the dermis of CD46 Tg and non-Tg mice, higher numbers of inflammatory cells were observed in the non-Tg mice (Fig. 3B and E). In addition, exfoliation of epidermis with intracellular edema and hemorrhaging in the dermis developed in CD46 Tg mice (Fig. 3B). At 48 h postinfection, the necrotic striated muscle layers were recognized in the dermis of CD46 Tg mice (Fig. 3C). In contrast, although the exfoliation of epidermis was observed, the necrosis could not yet be detected in the dermis of non-Tg mice at this stage (Fig. 3F).

These findings suggest that s.c. infection with GAS472 rapidly led to severe NF in the feet of CD46 Tg mice.

s.c. infection with GAS472 had a 100% mortality rate in CD46 Tg mice. As shown in Fig. 4, we observed differences in susceptibility of CD46 Tg mice after infection with 11 GAS strains. As a result, the mortality rates of the 336-h observation period were ranked in the following order: GAS472 (100%) > RE335 (83%) > GAS467 (67%) > RE025 (50%) > RE157 = GAS453 (43%) > GAS465 = RE137 (29%) > RE303 = RE386 = RE344 (0%). Therefore, we chose GAS472, RE335, and GAS467 as the three most virulent of the 11 GAS strains concerning the susceptibility of CD46 Tg mice. We then newly infected CD46 Tg and non-Tg mice with GAS472, RE335, or GAS467 at the same time. As shown in Fig. 5, the mortality rates among non-Tg mice were extremely low (0 or 10%). The differences in mortality rates between C57BL/6 and B6C3F1 mice after infection with each GAS strain were almost negligible. Thus, GAS472 was regarded as the most virulent strain in terms of the progression of NF and the susceptibility of CD46 Tg mice among 11 GAS strains.

s.c. infection with GAS472 was associated with a high level of bacterial load in deep tissues of CD46 Tg mice. As shown in Fig. 6, CD46 Tg mice had a significantly higher number of viable bacteria in each blood, spleen, and liver sample compared with non-Tg mice 48 h after infection with GAS472. Thereafter, the viable bacterial numbers in the blood and in every tissue sample increased 72 h after infection in CD46 Tg mice. Especially, the number of bacteria increased 90-fold in the livers of CD46 Tg mice for 24 h from 48 h to 72 h postinfection. In contrast, the number of bacteria increased sevenfold in the livers of non-Tg mice for 24 h from 48 h to 72 h postinfection. In other words, the estimated bacterial doubling

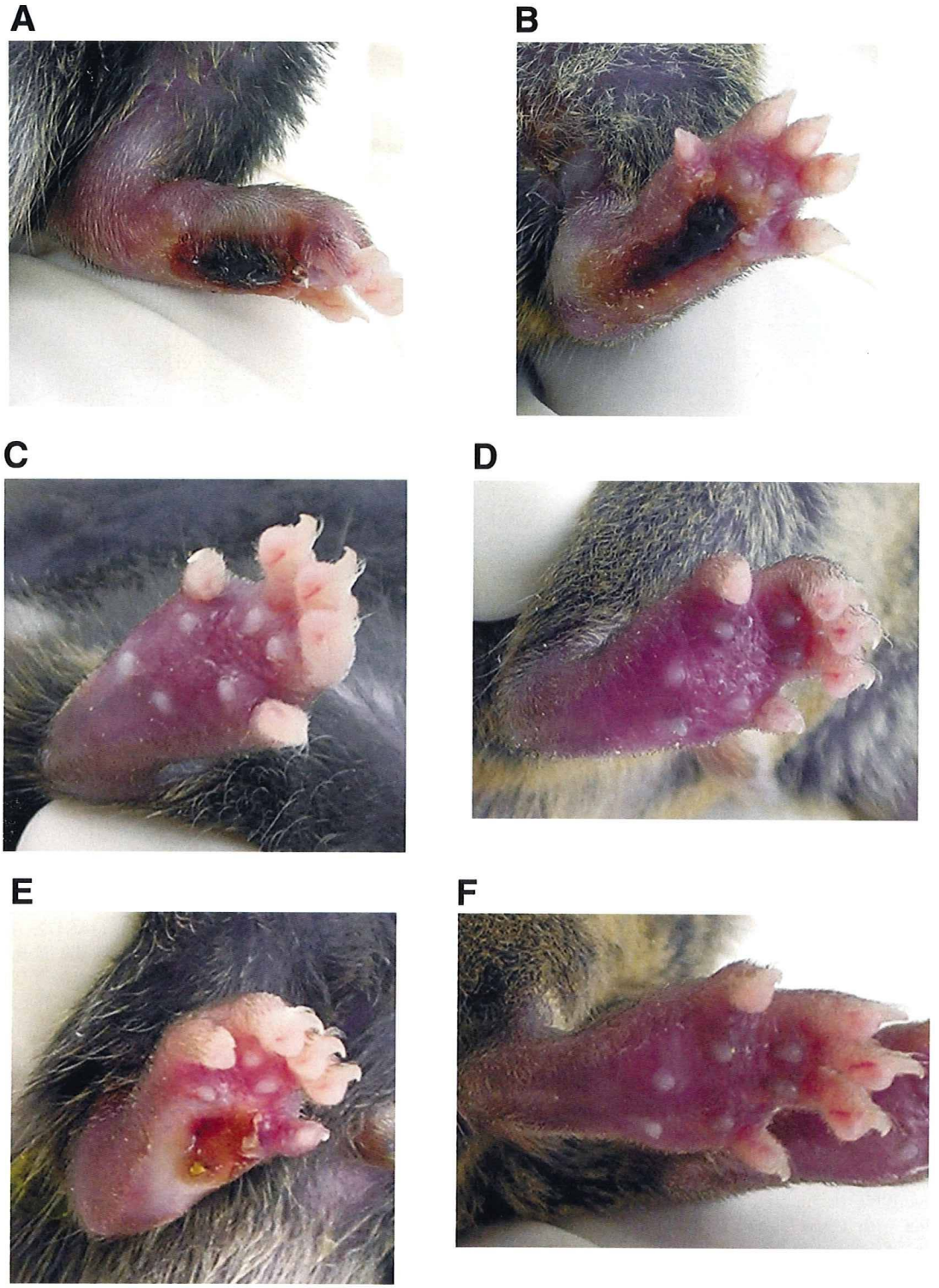

FIG. 2. Representative appearance of mild cutaneous lesions of non-Tg mouse feet. Shown is the macroscopic observation of C57BL/6 (A, C, and E) or B6C3F1 (B, D, and F) mouse foot 72 h after s.c. infection with 5×10^6 CFU of GAS strain GAS472 (A and B), GAS467 (C and D), or RE335 (E and F) per footpad.

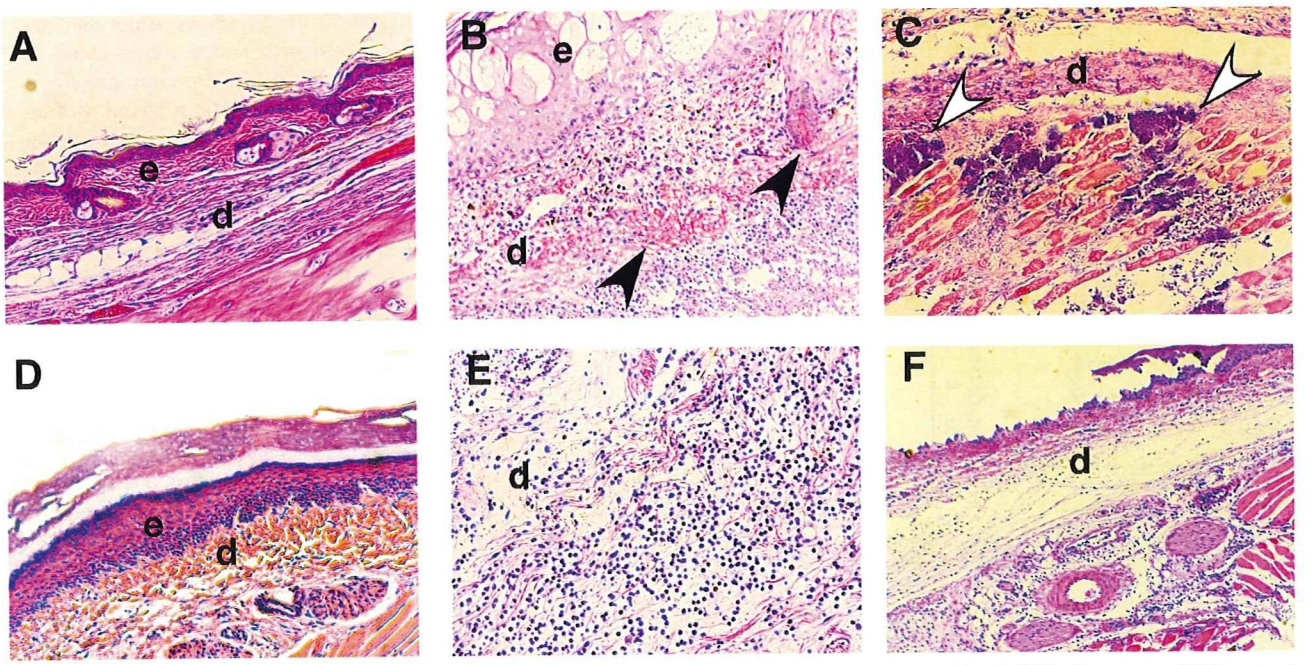

FIG. 3. Histological observation of footpad skin of CD46 Tg and non-Tg mice after s.c. infection with GAS472. Shown are H&E-stained footpad skin sections from CD46 Tg (A to C) and C57BL/6 (D to F) mice after s.c. infection with 5×10^6 CFU of GAS472 per footpad. (A and D) Uninfected. Original magnification, × 100. (B and E) Twenty-four hours after infection. Original magnification, ×200. (C and F) Forty-eight hours after infection. Original magnification, ×100. The closed arrowheads indicate hemorrhaging in the dermis. The open arrowheads indicate the necrotic striated muscle layers. e, epidermis; d, dermis.

times during these 24 h were 3.7 h and 8.5 h in the livers of CD46 Tg and non-Tg mice, respectively.

s.c. infection with GAS472 induced hepatic damage in CD46 Tg mice. Macroscopic observations showed the development of granulomatous nodules in the CD46 Tg mouse liver 72 h after s.c. infection with GAS472 (Fig. 7A). Simultaneously, microscopic observations revealed the development of full porous cytoplasmic F-actin bundles (Fig. 7C) in the liver sections of CD46 Tg mice after infection. Multifocal areas of necrosis were associated with inflammatory infiltrate (Fig. 7D), and clusters of streptococci were visible at the edges of the necrotic areas (Fig. 7E) in the liver sections of CD46 Tg mice after infection. Based on these results, we considered it likely that s.c. infection with GAS472 induced hepatic damage in CD46 Tg mice along with NF in their feet.

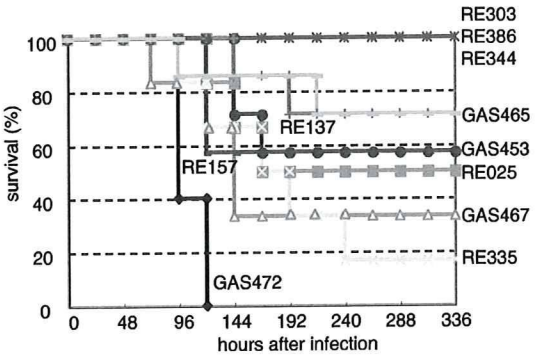

FIG. 4. Comparison of survival curves of CD46 Tg mice after s.c. infection with GAS strains. The mice infected s.c. with 5×10^6 CFU of GAS strains per footpad were monitored every 24 h for survival during the 336-h study. $n = 7$ for GAS453, RE137, RE157, and GAS465; $n = 6$ for RE335, GAS467, RE025, RE303, RE344, and RE386; and $n = 5$ for GAS472.

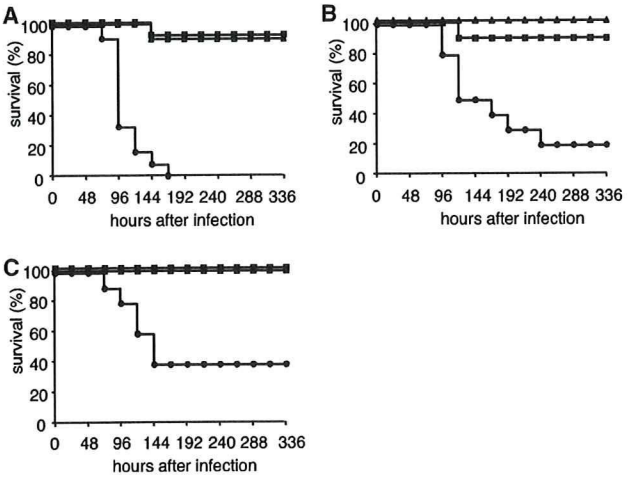

FIG. 5. Comparison of survival rates between CD46 Tg and non-Tg mice after s.c. infection with GAS strains. CD46 Tg and non-Tg (C57BL/6 and B6C3F1) mice were infected s.c. with 5×10^6 CFU of GAS472 (A), RE335 (B), or GAS467 (C) per footpad. The mice were then monitored every 24 h for survival during the 336-h study. Closed circles, CD46 Tg mice (A, $n = 12$; B and C, $n = 10$); closed squares, C57BL/6 mice (A, $n = 12$; B and C, $n = 10$); closed triangles, B6C3F1 mice (A and C, $n = 11$; B, $n = 10$).

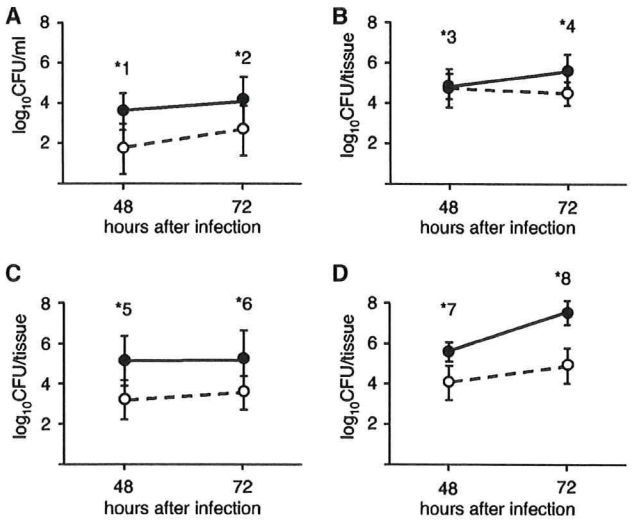

FIG. 6. Comparison of growth rates of GAS472 in the blood, PLN, spleen, and liver of mice. CD46 Tg (closed circles) and C57BL/6 (open circles) mice were infected s.c. with 5×10^6 CFU of GAS472 per footpad. At 48 and 72 h postinfection, the numbers of bacteria in the blood (A), PLN (B), spleen (C), and liver (D) samples were determined by plating. Data represent the mean value of the number of bacteria per ml (blood) or per tissue sample (PLN, spleen, and liver) ± SD. *1, $P = 0.001$; *2, $P = 0.02$; *3, $P = 0.77$; *4, $P = 0.002$; *5, $P = 0.001$; *6, $P = 0.008$; *7, $P = 0.00009$; *8, $P = 0.0000003$ (CD46 Tg mice versus non-Tg mice; $n = 10$).

Expression of *sagA* in GAS472 was increased when the bacterial cell suspension was mixed with mouse whole blood. It was demonstrated that during 6 h of incubation, the growth of GAS was enhanced in the cell culture medium mixed with an equal volume of mouse whole blood containing soluble human CD46 (30). Then, we examined the changes in expression of *sagA* (streptolysin S; SLS) of GAS472 during 6 h of incubation under the above experimental conditions. As shown in Fig. 8, ~3-, 30-, and 30-fold increases in expression of *sagA* were detected during the 1-, 2-, and 6-h incubations, respectively, with CD46 Tg mouse blood. In contrast, *sagA* increases in expression of about three-, seven-, and seven-fold were detected during the 1-, 2-, and 6-h incubations, respectively, with non-Tg mouse blood. Thus, progressive increases in the expression of *sagA* detected during the 2-h and 6-h incubations were CD46 Tg mouse blood dependent. The differences were not significant (P values of >0.05), although the expression levels of the CD46 Tg mouse blood-dependent group were higher than those of the non-Tg mouse blood-dependent group in all three of the experiments. Although we also examined for changes in gene expression of *emm* (M protein), *csrS* (sensor histidine kinase), *scpA* (C5a peptidase), *scpC* (serine protease), *ska* (streptokinase), *speB* (cystein protease), and *speA* (streptococcal pyrogenic exotoxin A) using real-time RT-PCR with each gene-specific primer pair, significant changes in gene expression were not detected during the 6-h incubation with CD46 Tg or non-Tg mouse blood.

In the meantime, it was also demonstrated that CsrRS (a

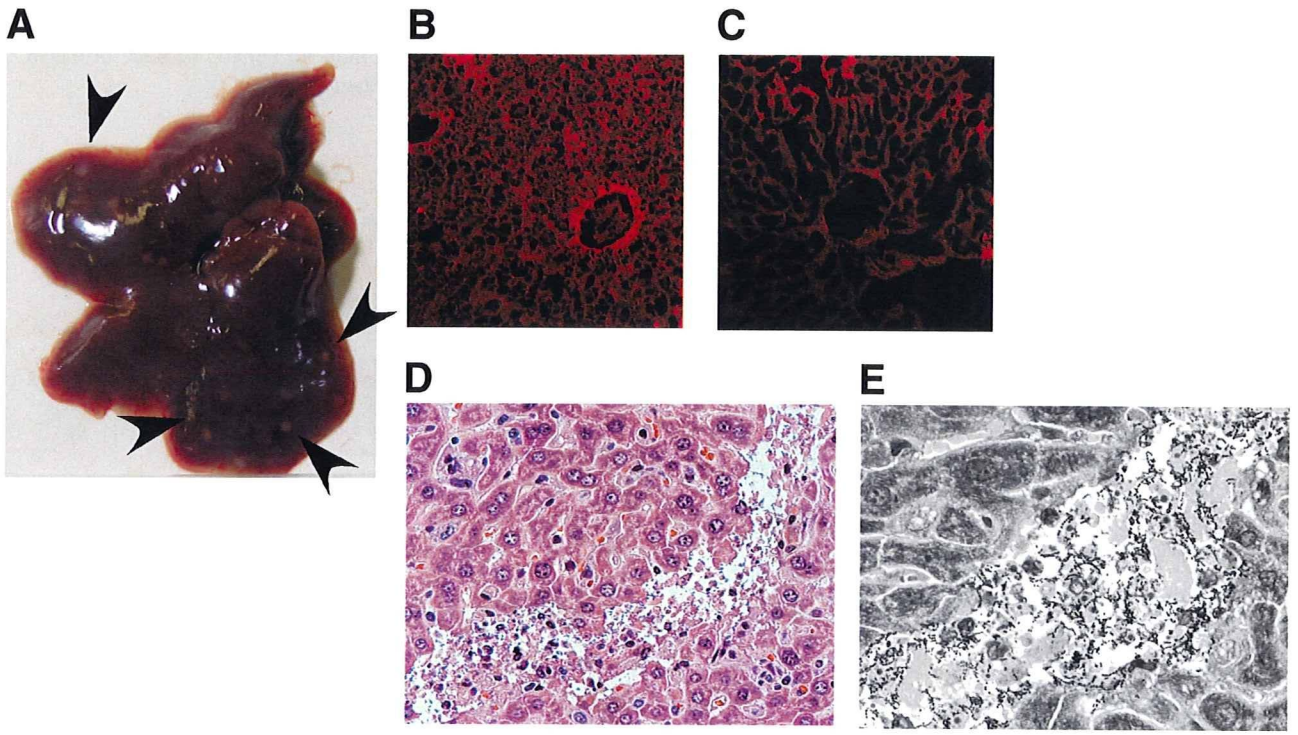

FIG. 7. Representative appearance of the liver and liver sections of CD46 Tg mice. Shown are a macroscopic observation of liver (A), a fluorescent phalloidin F-actin staining image (red) of a liver section (C), an H&E-stained liver section (D), and a Giemsa-stained liver section (E) of a CD46 Tg mouse 72 h after s.c. infection with 5×10^6 CFU of GAS472 per footpad. The immunofluorescence image of a liver section from an uninfected CD46 Tg mouse (B) is also shown. B, C, D, and E, original magnifications ×100, ×100, ×200, and ×400, respectively. The arrowheads indicate the granulomatous nodules in the liver.

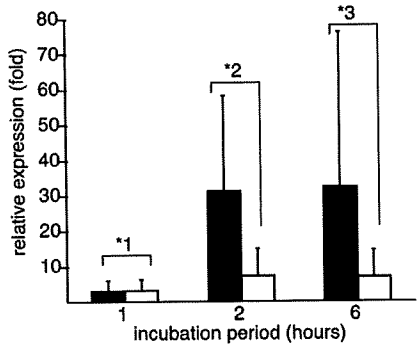

FIG. 8. Gene expression profile of GAS472 during the incubation period. Total RNA was prepared from bacterial cells, and quantitative real-time RT-PCR was carried out as described in Materials and Methods. At each time point, the expressional level of *sagA* was normalized to the corresponding 16S rRNA gene value. In addition, each normalized value was then converted to reflect the amplification of each value for zero time. Data represent the mean values ± SDs of three independent experiments. Closed columns, bacterial cell suspension with CD46 Tg mouse blood; open columns, bacterial cell suspension with C57BL/6 mouse blood. *1, $P = 0.25$; *2, $P = 0.08$; *3, $P = 0.17$ (CD46 Tg mouse blood versus non-Tg mouse blood).

member of the two-component regulatory system) influenced the transcription of 15% of all chromosomal genes of GAS, including negative controls on the gene expression of five virulence factors (capsule, cystein protease, streptokinase, SLS, and streptodornase) (18). Since recent studies showed that the mutation of *csrRS* was important for the invasive phenotype of GAS (2, 45), we compared the DNA sequences of *csrRS* among two virulent strains (GAS472 and GAS467), two avirulent strains (RE386 and RE344), and a type strain of GAS serotype M1 (MGAS5005). No DNA sequence variations were identified inside the coding regions of *csrRS* among GAS472 (accession no. AB513958), GAS467 (accession no. AB513957), RE386 (accession no. AB513956), RE344 (accession no. AB513955), and MGAS5005 (accession no. NC_007297). Instead, the following two variations were found in the 5′ noncoding regions of *csrRS*: variation 1, c.−55_−56insT (a single nucleotide insertion of T in GAS472, GAS467, RE386, and RE344 at the position between −55 and −56 from the TTG initiation codon of *csrS* in MGAS5005); and variation 2, c.−232delA (a single nucleotide deletion of A in GAS472 at position −232 from the ATG initiation codon of *csrR* in MGAS5005).

DISCUSSION

In human patients, NF due to GAS infection is defined pathologically by a deep-seated infection of the s.c. tissue that results in the progressive destruction of fascia and fat, with relative sparing of skeletal muscle (4, 13, 16, 28). NF is rare in young children but more common in otherwise healthy adults, in whom a minor skin wound often precedes the disease, as was reported in a case study of a 25-year-old man (13). That study showed extensive bands of liquefactive necrosis and patchy inflammation of the deep dermis and subcutis in specimens of the patient's skin and soft tissue (13). Moreover, a focal abscess with numerous degenerating neutrophils formed in the deep dermis in that case (13). These symptoms closely resemble the skin specimens of CD46 Tg mice after s.c. infection with GAS472, as described in Fig. 3.

In previously published mouse models of skin and soft tissue infection with GAS, the bacteria were inoculated s.c. into the backs (8, 32, 36), haunches (6), or flanks (1, 5, 7, 38). Compared to such models, the s.c. inoculation into both hind footpads in the present study was a simple procedure, and the obtained data showed a narrow dispersion of reproducibility. A recent study demonstrated that infection in epithelial cells with GAS led to the shedding of human CD46 at the same time as bacterium-induced apoptosis and cell death occurred (30). In the present study, the amount of bacterial load in the PLN of CD46 Tg mice was the same as that of non-Tg mice 48 h after s.c. infection (Fig. 6B), indicating that the same amounts of bacteria resided in the feet of CD46 Tg and non-Tg mice for 48 h after s.c. infection. However, since the progression of NF until 48 h after s.c. infection was dramatically elevated in the feet of CD46 Tg mice compared to those of non-Tg mice (Fig. 3), human CD46-mediated GAS infection was thought to be necessary for the observed acceleration of disease progression in the mouse feet. Interestingly, in many cases, non-Tg mouse feet were completely extinguished by persistent necrosis of skin, soft tissue, and bone up to 336 h after infection with GAS472, although the mice were still alive (Fig. 9A). In addition, the majority of CD46 Tg mouse feet were also lost by persistent necrosis no later than 336 h after infection with even avirulent GAS strains other than GAS472, GAS467, and RE025 (Fig. 9B). Possibly, such persistent necrosis due to GAS infection cannot lead to death in CD46 Tg and non-Tg mice.

We classified 11 clinical isolates into the virulent or avirulent strains of GAS based on the severity levels of foot lesions at 72 h and the mortality rates by 336 h after s.c. infection. RE303 and RE344 did not show the capacity to induce lethal disease in CD46 Tg mice (Fig. 4), despite the fact that they were recovered from patients with invasive diseases (Table 1). In both cases, the patients were immunocompromised due to preexisting diseases. Supposedly, even avirulent GAS strains are able to induce invasive diseases in the patients suffering from preexisting medical conditions.

According to a previous report, GAS infection was commonly associated with the early onset of shock and organ failure in humans (4). Another recent study demonstrated that GAS might bind available extracellular CD46 as a strategy to survive and avoid host defenses and that the lethal disease and arthritis were much more frequent in CD46 Tg mice than in non-Tg mice after i.v. infection with GAS (30). Our data clearly indicate that the proliferation rate during the 24 h between 48 and 72 h after s.c. infection with GAS472 in the liver was much higher in CD46 Tg mice than in non-Tg mice (Fig. 6D). Indeed, bacterial infection induced serious liver damage in CD46 Tg mice (Fig. 7). Probably, human CD46 potentially ensures bacterial growth in the deep tissues. Thereafter, systemic GAS infection might lead to organ failure and ultimately to the death of the mice.

The M proteins appear as long, hairlike filaments on the bacterial surface and are composed of two α-helical chains that are predominantly arranged in a coiled-coil conformation (14). All of the M proteins contain a conserved C-terminal region near the cell surface and a hypervariable N-terminal region

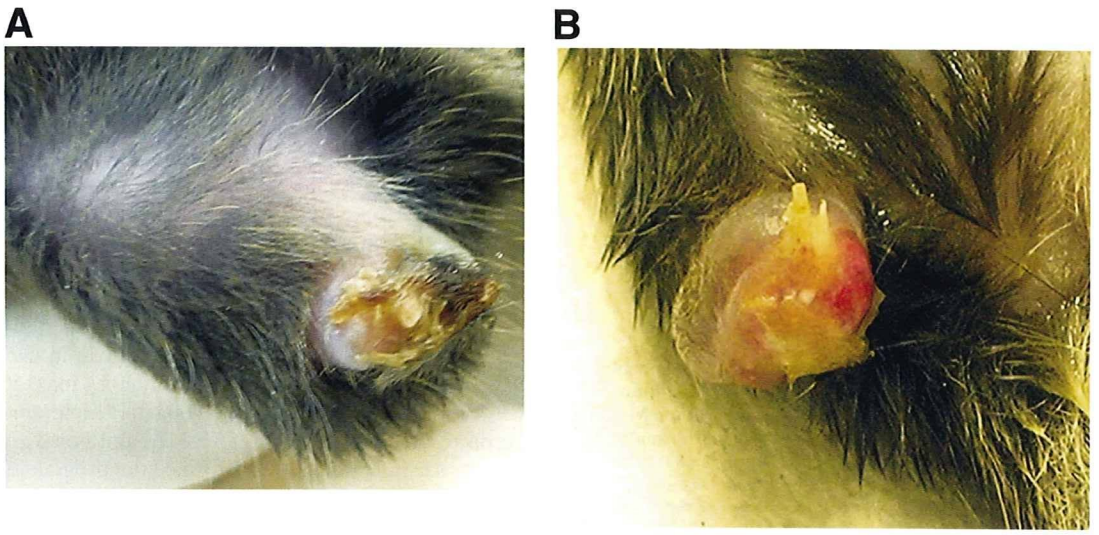

FIG. 9. Ultimate appearance of the mouse feet. Shown is a macroscopic observation of a C57BL/6 (A) or CD46 Tg (B) mouse foot 336 h after s.c. infection with 5×10^6 CFU of GAS472 or RE137 per footpad, respectively.

that provides the basis for serological typing (14). A function of M proteins was shown to be critical for protecting organisms from phagocytosis (14). An in vitro invasion study using A549 human lung epithelial cells demonstrated that the M protein-promoted ingestion of GAS was dependent on the coengagement of CD46 and α5β1 integrin (39). In addition, CD46-mediated invasion was also found to depend on the extracellular matrix protein fibronectin (39). CD46 has been generally recognized as a regulator of the complement system that facilitates factor I-mediated inactivation of the activated complement proteins C3b and C4b (29). In the meanwhile, the interaction between GAS and CD46 triggered cell signaling pathways that directly induced an immunosuppressive phenotype in T cells (26). In fact, by immunohistochemistry, M protein/fibrinogen complexes were identified in tissue biopsies from a patient suffering from NF and STSS (19). Recently, it was shown that the binding of CD46 to GAS serotype M18 strains was independent of Emm (M protein) or Enn (immunoglobulin A-binding protein) (12). There may be some biological advantages to GAS having Emm-dependent and Emm-independent CD46-binding abilities. In any case, whether or not the M1 protein directly responded to human CD46 in the host cell, we suppose that the human CD46-dependent regulation of virulence gene expression in GAS serotype M1 strains should be necessary for the induction of both local inflammation and deep tissue damage in the CD46 Tg mouse model.

It is well known that ScpC can cleave interleukin-8, a chemokine that mediates neutrophil transmission and activation (10, 20). The ScpC mutant strain did not degrade interleukin-8 and thus failed to prevent recruitment of immune cells; also, it caused disease after soft tissue infection (43), whereas the increased expression of ScpC and streptolysin O (a membrane-damaging extracellular toxin) caused by *csrS* mutation played a prominent role in the mouse model of GAS infection (2). Meanwhile, since GAS serotype M1 strains isolated from invasive diseases in human had mutation accumulation at the *csrRS* locus, resulting in an SpeB-negative phenotype (45), the SpeB expression levels of GAS serotype M1 strains were thought to be inversely correlated with disease severity in humans (24). In fact, an SpeB-negative phenotype caused by the *csrRS* mutation was a more virulent strain of GAS than the wild-type strain in the mouse model (47). Consequently, we had expected that GAS472 gained any mutation inside the coding regions of *csrRS* during infection, resulting in the high-virulence phenotype. Against our expectation, no DNA sequence variation was found inside the coding regions of *csrRS* in virulent strains (GAS472 and GAS467) or avirulent strains (RE344 and RE386) compared to a standard strain (MGAS5005). Unexpectedly, however, it became clear that the high-virulence phenotypes were not due to the mutation of *csrRS*. Therefore, the most significant questions—regarding genetic differences and virulence genes in different strains and how the virulent strains cause serious and lethal disease in humans—remain unanswered.

ACKNOWLEDGMENTS

We are grateful to John P. Atkinson for kindly providing the CD46 Tg mouse strain.

This work was financially supported by a grant under the category "Research Projects for Emerging and Re-emerging Infectious Diseases" (H-19-002 and H-20-002) from the Ministry of Health, Labor and Welfare of Japan.

We declare that no conflict of interest exists.

REFERENCES

1. **Ashbaugh, C. D., H. B. Warren, V. J. Carey, and M. R. Wessels.** 1998. Molecular analysis of the role of the group A streptococcal cysteine protease, hyaluronic acid capsule, and M protein in a murine model of human invasive soft-tissue infection. J. Clin. Investig. **102:**550–560.
2. **Ato, M., T. Ikebe, H. Kawabata, T. Takemori, and H. Watanabe.** 2008. Incompetence of neutrophils to invasive group A streptococcus is attributed to induction of plural virulence factors by dysfunction of a regulator. PLoS ONE **3:**e3455.
3. **Aziz, R. K., and M. Kotb.** 2008. Rise and persistence of global M1T1 clone of *Streptococcus pyogenes*. Emerg. Infect. Dis. **14:**1511–1517.
4. **Bisno, A. L., and D. L. Stevens.** 1996. Streptococcal infections of skin and soft tissues. N. Engl. J. Med. **334:**240–245.
5. **Brenot, A., K. Y. King, B. Janowiak, O. Griffith, and M. G. Caparon.** 2004.

Contribution of glutathione peroxidase to the virulence of *Streptococcus pyogenes*. Infect. Immun. **72**:408–413.
6. **Dalton, T. L., R. I. Hobb, and J. R. Scott.** 2006. Analysis of the role of CovR and CovS in the dissemination of *Streptococcus pyogenes* in invasive skin disease. Microb. Pathog. **40**:221–227.
7. **Datta, V., S. M. Myskowski, L. A. Kwinn, D. N. Chiem, N. Varki, R. G. Kansal, M. Kotb, and V. Nizet.** 2005. Mutational analysis of the group A streptococcal operon encoding streptolysin S and its virulence role in invasive infection. Mol. Microbiol. **56**:681–695.
8. **Di Nardo, A., K. Yamasaki, R. A. Dorschner, Y. Lai, and R. L. Gallo.** 2008. Mast cell cathelicidin antimicrobial peptide prevents invasive group A *Streptococcus* infection of the skin. J. Immunol. **180**:7565–7573.
9. **Dorig, R. E., A. Marcil, A. Chopra, and C. D. Richardson.** 1993. The human CD46 molecule is a receptor for measles virus (Edmonston strain). Cell **75**:295–305.
10. **Edwards, R. J., G. W. Taylor, M. Ferguson, S. Murray, N. Rendell, A. Wrigley, Z. Bai, J. Boyle, S. J. Finney, A. Jones, H. H. Russell, C. Turner, J. Cohen, L. Faulkner, and S. Sriskandan.** 2005. Specific C-terminal cleavage and inactivation of interleukin-8 by invasive disease isolates of *Streptococcus pyogenes*. J. Infect. Dis. **192**:783–790.
11. **Eguchi, M., Y. Sekiya, M. Suzuki, T. Yamamoto, and H. Matsui.** 2007. An oral *Salmonella* vaccine promotes the down-regulation of cell surface Toll-like receptor 4 (TLR4) and TLR2 expression in mice. FEMS Immunol. Med. Microbiol. **50**:300–308.
12. **Feito, M. J., A. Sanchez, M. A. Oliver, D. Perez-Caballero, S. Rodriguez de Cordoba, S. Alberti, and J. M. Rojo.** 2007. Membrane cofactor protein (MCP, CD46) binding to clinical isolates of *Streptococcus pyogenes*: binding to M type 18 strains is independent of Emm or Enn proteins. Mol. Immunol. **44**:3571–3579.
13. **Filbin, M. R., D. C. Ring, M. R. Wessels, L. L. Avery, and R. L. Kradin.** 2009. Case records of the Massachusetts General Hospital. Case 2-2009. A 25-year-old man with pain and swelling of the right hand and hypotension. N. Engl. J. Med. **360**:281–290.
14. **Fischetti, V. A.** 1989. Streptococcal M protein: molecular design and biological behavior. Clin. Microbiol. Rev. **2**:285–314.
15. **Fischetti, V. A., K. F. Jones, S. K. Hollingshead, and J. R. Scott.** 1988. Structure, function, and genetics of streptococcal M protein. Rev. Infect. Dis. **10**(Suppl. 2):S356–S359.
16. **Fustes-Morales, A., P. Gutierrez-Castrellon, C. Duran-Mckinster, L. Orozco-Covarrubias, L. Tamayo-Sanchez, and R. Ruiz-Maldonado.** 2002. Necrotizing fasciitis: report of 39 pediatric cases. Arch. Dermatol. **138**:893–899.
17. **Gaggar, A., D. M. Shayakhmetov, and A. Lieber.** 2003. CD46 is a cellular receptor for group B adenoviruses. Nat. Med. **9**:1408–1412.
18. **Graham, M. R., L. M. Smoot, C. A. Migliaccio, K. Virtaneva, D. E. Sturdevant, S. F. Porcella, M. J. Federle, G. J. Adams, J. R. Scott, and J. M. Musser.** 2002. Virulence control in group A *Streptococcus* by a two-component gene regulatory system: global expression profiling and in vivo infection modeling. Proc. Natl. Acad. Sci. USA **99**:13855–13860.
19. **Herwald, H., H. Cramer, M. Morgelin, W. Russell, U. Sollenberg, A. Norrby-Teglund, H. Flodgaard, L. Lindbom, and L. Bjorck.** 2004. M protein, a classical bacterial virulence determinant, forms complexes with fibrinogen that induce vascular leakage. Cell **116**:367–379.
20. **Hidalgo-Grass, C., M. Dan-Goor, A. Maly, Y. Eran, L. A. Kwinn, V. Nizet, M. Ravins, J. Jaffe, A. Peyser, A. E. Moses, and E. Hanski.** 2004. Effect of a bacterial pheromone peptide on host chemokine degradation in group A streptococcal necrotising soft-tissue infections. Lancet **363**:696–703.
21. **Johansson, L., A. Rytkonen, P. Bergman, B. Albiger, H. Kallstrom, T. Hokfelt, B. Agerberth, R. Cattaneo, and A. B. Jonsson.** 2003. CD46 in meningococcal disease. Science **301**:373–375.
22. **Johansson, L., A. Rytkonen, H. Wan, P. Bergman, L. Plant, B. Agerberth, T. Hokfelt, and A. B. Jonsson.** 2005. Human-like immune responses in CD46 transgenic mice. J. Immunol. **175**:433–440.
23. **Kallstrom, H., M. K. Liszewski, J. P. Atkinson, and A. B. Jonsson.** 1997. Membrane cofactor protein (MCP or CD46) is a cellular pilus receptor for pathogenic *Neisseria*. Mol. Microbiol. **25**:639–647.
24. **Kansal, R. G., A. McGeer, D. E. Low, A. Norrby-Teglund, and M. Kotb.** 2000. Inverse relation between disease severity and expression of the streptococcal cysteine protease, SpeB, among clonal M1T1 isolates recovered from invasive group A streptococcal infection cases. Infect. Immun. **68**:6362–6369.
25. **Kemper, C., M. Leung, C. B. Stephensen, C. A. Pinkert, M. K. Liszewski, R. Cattaneo, and J. P. Atkinson.** 2001. Membrane cofactor protein (MCP; CD46) expression in transgenic mice. Clin. Exp. Immunol. **124**:180–189.
26. **Kemper, C., J. W. Verbsky, J. D. Price, and J. P. Atkinson.** 2005. T-cell stimulation and regulation: with complements from CD46. Immunol. Res. **32**:31–43.
27. **Kodama, C., M. Eguchi, Y. Sekiya, T. Yamamoto, Y. Kikuchi, and H. Matsui.** 2005. Evaluation of the Lon-deficient *Salmonella* strain as an oral vaccine candidate. Microbiol. Immunol. **49**:1035–1045.
28. **Leitch, H. A., A. Palepu, and C. M. Fernandes.** 2000. Necrotizing fasciitis secondary to group A streptococcus. Morbidity and mortality still high. Can. Fam. Physician **46**:1460–1466.
29. **Liszewski, M. K., T. W. Post, and J. P. Atkinson.** 1991. Membrane cofactor protein (MCP or CD46): newest member of the regulators of complement activation gene cluster. Annu. Rev. Immunol. **9**:431–455.
30. **Lövkvist, L., H. Sjölinder, R. Wehelie, H. Aro, A. Norrby-Teglund, L. Plant, and A.-B. Jonsson.** 2008. CD46 contributes to the severity of group A streptococcal infection. Infect. Immun. **76**:3951–3958.
31. **Manchester, M., M. K. Liszewski, J. P. Atkinson, and M. B. Oldstone.** 1994. Multiple isoforms of CD46 (membrane cofactor protein) serve as receptors for measles virus. Proc. Natl. Acad. Sci. USA **91**:2161–2165.
32. **Medina, E., O. Goldmann, A. W. Toppel, and G. S. Chhatwal.** 2003. Survival of *Streptococcus pyogenes* within host phagocytic cells: a pathogenic mechanism for persistence and systemic invasion. J. Infect. Dis. **187**:597–603.
33. **Miyoshi-Akiyama, T., J. Zhao, K. Kikuchi, H. Kato, R. Suzuki, M. Endoh, and T. Uchiyama.** 2003. Quantitative and qualitative comparison of virulence traits, including murine lethality, among different M types of group A streptococci. J. Infect. Dis. **187**:1876–1887.
34. **Mrkic, B., J. Pavlovic, T. Rülicke, P. Volpe, C. J. Buchholz, D. Hourcade, J. P. Atkinson, A. Aguzzi, and R. Cattaneo.** 1998. Measles virus spread and pathogenesis in genetically modified mice. J. Virol. **72**:7420–7427.
35. **Naniche, D., G. Varior-Krishnan, F. Cervoni, T. F. Wild, B. Rossi, C. Rabourdin-Combe, and D. Gerlier.** 1993. Human membrane cofactor protein (CD46) acts as a cellular receptor for measles virus. J. Virol. **67**:6025–6032.
36. **Nizet, V., T. Ohtake, X. Lauth, J. Trowbridge, J. Rudisill, R. A. Dorschner, V. Pestonjamasp, J. Piraino, K. Huttner, and R. L. Gallo.** 2001. Innate antimicrobial peptide protects the skin from invasive bacterial infection. Nature **414**:454–457.
37. **Okada, N., M. K. Liszewski, J. P. Atkinson, and M. Caparon.** 1995. Membrane cofactor protein (CD46) is a keratinocyte receptor for the M protein of the group A streptococcus. Proc. Natl. Acad. Sci. USA **92**:2489–2493.
38. **Peyssonnaux, C., A. S. Zinkernagel, V. Datta, X. Lauth, R. S. Johnson, and V. Nizet.** 2006. TLR4-dependent hepcidin expression by myeloid cells in response to bacterial pathogens. Blood **107**:3727–3732.
39. **Rezcallah, M. S., K. Hodges, D. B. Gill, J. P. Atkinson, B. Wang, and P. P. Cleary.** 2005. Engagement of CD46 and α5β1 integrin by group A streptococci is required for efficient invasion of epithelial cells. Cell. Microbiol. **7**:645–653.
40. **Santoro, F., P. E. Kennedy, G. Locatelli, M. S. Malnati, E. A. Berger, and P. Lusso.** 1999. CD46 is a cellular receptor for human herpesvirus 6. Cell **99**:817–827.
41. **Segerman, A., J. P. Atkinson, M. Marttila, V. Dennerquist, G. Wadell, and N. Arnberg.** 2003. Adenovirus type 11 uses CD46 as a cellular receptor. J. Virol. **77**:9183–9191.
42. **Sjolinder, H., and A. B. Jonsson.** 2007. Imaging of disease dynamics during meningococcal sepsis. PLoS ONE **2**:e241.
43. **Sjölinder, H., L. Lövkvist, L. Plant, J. Eriksson, H. Aro, A. Jones, and A.-B. Jonsson.** 2008. The ScpC protease of *Streptococcus pyogenes* affects the outcome of sepsis in a murine model. Infect. Immun. **76**:3959–3966.
44. **Stefanini, M., C. De Martino, and L. Zamboni.** 1967. Fixation of ejaculated spermatozoa for electron microscopy. Nature **216**:173–174.
45. **Sumby, P., A. R. Whitney, E. A. Graviss, F. R. DeLeo, and J. M. Musser.** 2006. Genome-wide analysis of group A streptococci reveals a mutation that modulates global phenotype and disease specificity. PLoS Pathog. **2**:e5.
46. **Tewodros, W., and G. Kronvall.** 2005. M protein gene (*emm* type) analysis of group A beta-hemolytic streptococci from Ethiopia reveals unique patterns. J. Clin. Microbiol. **43**:4369–4376.
47. **Walker, M. J., A. Hollands, M. L. Sanderson-Smith, J. N. Cole, J. K. Kirk, A. Henningham, J. D. McArthur, K. Dinkla, R. K. Aziz, R. G. Kansal, A. J. Simpson, J. T. Buchanan, G. S. Chhatwal, M. Kotb, and V. Nizet.** 2007. DNase Sda1 provides selection pressure for a switch to invasive group A streptococcal infection. Nat. Med. **13**:981–985.
48. **Wu, E., S. A. Trauger, L. Pache, T.-M. Mullen, D. J. von Seggern, G. Siuzdak, and G. R. Nemerow.** 2004. Membrane cofactor protein is a receptor for adenoviruses associated with epidemic keratoconjunctivitis. J. Virol. **78**:3897–3905.

Editor: J. N. Weiser

RESEARCH LETTER

Positive correlation between low adhesion of group A *Streptococcus* to mammalian cells and virulence in a mouse model

Tohru Miyoshi-Akiyama[1], Jizi Zhao[1,2], Takehiko Uchiyama[3], Junji Yagi[3] & Teruo Kirikae[1]

[1]Department of Infectious Diseases, International Medical Center of Japan, Research Institute, Toyama, Shinjuku-ku, Tokyo, Japan; [2]Department of Special Pathogen, International Research Center for Infectious Disease, Research Institute for Microbial Disease, Osaka University, Yamadaoka, Suita, Osaka, Japan; and [3]Department of Microbiology and Immunology, Tokyo Women's Medical University, Kawada-cho, Shinjuku-ku, Tokyo, Japan

Correspondence: Tohru Miyoshi-Akiyama, Department of Infectious Diseases, International Medical Center of Japan, Research Institute, 1-21-1, Toyama, Shinjuku-ku, Tokyo, 162-8655, Japan. Tel.: +81 3 3202 7181, ext. 2903; fax: +81 3 3202 7364; e-mail: takiyam@ri.imcj.go.jp

Received 10 October 2008; accepted 11 January 2009.
First published online 12 February 2009.

DOI:10.1111/j.1574-6968.2009.01513.x

Editor: Jan-Ingmar Flock

Keywords
Streptococcus; STSS; GAS; adhesin; *in vivo* model.

Abstract

We previously reported that a mouse model reflected, at least in part, the pathogenic mechanism of bacteremia observed during streptococcal toxic shock syndrome caused by group A *Streptococcus* (GAS). We have extended this study by assaying the *in vitro* adhesion of these same isolates to mammalian cells. Unexpectedly, we found that high-virulence GAS isolates in the mouse model showed low adhesion to the host cells. Similarly, the rate of recovery from the peritoneal cavity and cardiac blood of mice after intraperitonial injection was higher for high- than for low-virulence strains. Levels of expression of molecules that affect the adhesion of GAS to host cells were not significantly correlated with GAS virulence. Taken together, these results indicate that the invasiveness of GAS, reflected as higher virulence, is correlated directly with lower adhesion to host cells.

Introduction

The group A streptococci (GAS) cause various infectious disease, including invasive streptococcal toxic shock syndrome (STSS), which can be lethal (Smith *et al.*, 2005). Epidemiological studies have shown that GAS strains carrying *emm1* and *emm3* are more frequently isolated from STSS than strains carrying *emm4*, and *emm12*. Because GAS usually do not show significant virulence in mice, there has been no good mouse model reflecting the pathogenic mechanism of STSS. To analyze the pathogenic mechanism of GAS, we compared the virulence in mice of GAS clinical isolates carrying *emm1*, *emm3*, *emm4* and *emm12* by injecting these isolates into mouse peritoneal cavities. We found that GAS isolates carrying *emm1* and *emm3* showed higher virulence than those carrying *emm4* and *emm12*, indicating that this mouse model reflected, at least in part, the pathogenic mechanism of bacteremia observed during STSS (Shiseki *et al.*, 1999; Miyoshi-Akiyama *et al.*, 2003).

Adhesion of bacteria to the host cell is considered one of the most important processes in bacterial infection (Kerr, 1999; Raupach *et al.*, 1999). Many GAS products are known as adherence factors (Molinari *et al.*, 1997; Schrager & Wessels, 1997; Fluckiger *et al.*, 1998; Jadoun *et al.*, 1998; Terao *et al.*, 2001, 2002a; Mora *et al.*, 2005). Testing of the relationship between GAS adherence and virulence in animal models (Courtney *et al.*, 1994; Wessels & Bronze, 1994; Terao *et al.*, 2001, 2002b) has shown that, like other bacteria, GAS requires an adhesion step to colonize the host. In contrast to other types of GAS infection, GAS spreads rapidly throughout the body in individuals with STSS, making it likely that GAS causing STSS has particular features that allow it to interact with and adhere to the host cell.

While assessing our mouse model of STSS, we constructed a panel of GAS isolates with known virulence against mice following intraperitonial infection. In this study, we examined the adherence of these GAS isolates to mammalian cells. Unexpectedly, we found that isolates with higher virulence in mice showed lower adherence to mammalian cells. Our findings suggest that the adhesion of GAS to mammalian cells reduces virulence in our mouse model.

Materials and methods

Bacterial isolates and media

Profiles of GAS clinical isolates used in this study are summarized in Table 1. To prevent phenotypic changes of the isolates during passage, all isolates were stored at −80 °C until use. The GAS isolates were cultured in Brain–Heart Infusion broth (Difco) overnight in the presence of 5% CO_2 at 37 °C. The lethal dose 50% (LD_{50}) values indicated in Table 1 were based on our previous study (Shiseki *et al.*, 1999). In that study, GAS suspended at 0.5 mL of phosphate buffered saline (PBS) and fivefold serial dilutions was injected intraperitonially into female 6-week-old *ddY* mice (SLC Japan; 10 mice per group). The mice were observed for 3 days and the LD_{50} was calculated.

emm typing and pulsed-field gel electrophoresis (PFGE)

emm typing of the GAS isolates was performed as described (http://www.cdc.gov/ncidod/biotech/strep/strepindex.htm) with minor modifications. GAS isolates were compared by PFGE using a GenePath system (Bio-Rad) with SmaI digestion, as described (Miyoshi-Akiyama *et al.*, 2003).

GAS adhesion to mammalian cells

The mammalian cell lines used in this study included the mouse fibroblast cell line, L cells, as well as HeLa and HEp-2 cells. These cells were precultured overnight in 2 mL of Roswell Park Memorial Institute medium (RPMI) 1640 containing 10% fetal calf serum (FCS) at 1×10^5 cell per well in 24-well culture plates. One hour before using the cells, the medium was replaced with 1 mL of fresh RPMI 1640 containing 10% FCS. The concentrations of overnight cultures of GAS isolates were adjusted to an $OD_{600\,nm}$ of 0.02, and a 20-μL aliquot of each GAS suspension, containing *c.* 2×10^4 CFU of bacteria, was added to the mammalian cell cultures (MOI = 0.2). After 4 h of incubation in a humidified 5% CO_2 incubator at 37 °C, each well was washed five times with 1 mL of PBS, and 500 μL of DDW was added to disrupt the cells. After vortexing for 30 s, the suspensions were plated on duplicate sheep blood agar plates to determine the number of CFU. To analyze bacterial growth, the bacteria were recovered by centrifugation and the number was counted by plating as described above. To microscopically assay the adherence of GAS to L cells, the cells were cultured in chamber slides (Lab-Tek) with the GAS isolates, washed using the same conditions as described above, and the cells were subjected to conventional Giemsa staining.

Recovery of GAS from the abdominal cavity and bloodstream after intraperitonial injection

The $OD_{600\,nm}$ values of GAS isolates were adjusted to 2 and 20 with PBS for recovery from the peritoneal cavity and bloodstream, respectively, and 0.5 mL of each suspension was injected intraperitonial into *ddY* mice (four animals per GAS isolate). Under these conditions, *c.* 1×10^8 and

Table 1. Profiles of the GAS isolates in this study

Disease	Isolate name	Sites of isolation in mice	Fate of the patients	*emm* type	LD_{50} (CFU per mouse)*
STSS	ST1	Blood, pharynx	Recovered	*emm3*	8.33×10^3
	ST2	Blood, necrotic tissues	Died	*emm89*	2.51×10^5
	ST3	Blood, necrotic tissues	Died	*emm3*	1.12×10^6
	ST4	Blood, necrotic tissues	Died	*emm3*	2.51×10^6
	ST5	Pharynx	Recovered	*emm3*	9.97×10^6
	ST6	Blood	Died	*emm3*	1.68×10^6
	ST7	Blood	Died	*emm3*	6.31×10^7
	ST8	Blood	Recovered	*emm4*	7.94×10^7
	ST9	Blood, necrotic tissues	Died	*emm22.2*	2.51×10^8
	ST10	Blood, necrotic tissues	Died	*emm4*	5.53×10^7
Scarlet fever	SF1	Pharynx	Recovered	*emm1*	9.13×10^6
	SF2	Pharynx	Recovered	*emm13w*	2.51×10^8
	SF3	Pharynx	Recovered	*emm11*	2.82×10^8
	SF4	Pharynx	Recovered	*emm4*	3.55×10^8
	SF5	Pharynx	Recovered	*emm4*	3.98×10^8
	SF6	Pharynx	Recovered	*emm12*	4.47×10^8
	SF7	Pharynx	Recovered	*emm4*	5.01×10^8
	SF8	Pharynx	Recovered	*emm12*	1.80×10^7
	SF9	Pharynx	Recovered	*emm12*	1.25×10^7
	SF10	Pharynx	Recovered	*emm4*	3.36×10^7

*Based on Shiseki *et al.* (1999).

1×10^9 CFU per mouse were injected for recovery from the peritoneal cavity and bloodstream, respectively. The actual number of bacterial cells inoculated was confirmed by plating, as described above, and there was no significant difference among the isolates (data not shown). To recover bacterial cells from the peritoneal cavity, the latter was rinsed with 3 mL PBS 30 min after injection, and the collected PBS was used as the sample. To recover bacteria from the bloodstream, blood samples were obtained by cardiac puncture 3 h after injection. These samples were plated on sheep blood agar plates as described above.

Immunoblotting against M proteins

The constant region of the M6 protein gene was amplified by standard PCR using primers containing a BamHI site (5′-GGGAGGGGATCCGCATCACGTGAAGCTTAAGAAA-3′) and a SalI site (5′-AGTGGCGTCGACTTAGTTTTCT TCTTTGGGTTT-3′), and cloned into the corresponding sites of the his-tag expression vector, pQE30 (Qiagen). The resulting plasmid was introduced into *Escherichia coli* XL1-blue (Stratagene) and recombinant protein of the constant region of M6 was expressed using isopropyl-β-D-thiogalactopyranoside, and purified by affinity to Ni-chelate resin, as described by the manufacturers. The protein was further purified by cation-exchange column chromatography, and injected into rabbits using standard procedures. These antisera were used for immunoblotting. GAS isolates were cultured as above. After adjusting the bacterial cell number by measuring the OD, the cells were lysed in sodium dodecyl sulfate-polyacrylamide gel electrophoresis (SDS-PAGE) sample buffer and subjected to standard SDS-PAGE followed by electroblotting on polyvinylidene difluoride (PVDF) membranes (NEN Life Science Products). Proteins were visualized using ECL (GE healthcare).

Hyaluronic acid quantification

Quantification of the amount of hyaluronic acid in each GAS isolate, using Stains-All (Sigma-Aldrich), was performed as described (Miyoshi-Akiyama *et al.*, 2003).

Far-Western blotting using fibronectin as a probe

To compare the profile of fibronectin-interacting proteins produced by each GAS isolate, far-Western blotting was performed using fibronectin as a probe. PVDF filters blotted with GAS lysates were prepared as described above. The filters were incubated with 10 μg mL^{-1} of fibronectin (Upstate Biotechnology), and the binding of fibronectin to the GAS proteins was detected using rabbit antifibronectin polyclonal antibody (Biomedicals Inc.) with the chemiluminescence systems described above.

Statistical analysis

Data were analyzed for significance by the Kendall's rank correlation test for nonparametric data. These analyses were performed using STAT-MACROS for MS-EXCEL (http://www.tuat.ac.jp/~ethology/Columbo/Stat/index.html), and $P < 0.05$ was used to indicate statistical significance.

Results

PFGE pattern and *emm* type of the GAS isolates

When we analyzed the GAS isolates used in this study by PFGE after SmaI digestion, we found that their PFGE patterns agreed with those reported previously (Stanley *et al.*, 1995; Murase *et al.*, 1999) (Fig. 1). ST1 to ST7 showed the same PFGE pattern without any polymorphism, although the *emm* type of ST2, *emm89*, differs from the type, *emm3*, in ST1 and ST3 to ST7. Thus, ST1 to ST7 have similar genetic backgrounds. The other isolates with *emm4* (ST8, ST10, SF4, SF5, SF7, and SF10) or *emm12* (SF6, SF8, and SF9) showed PFGE patterns that differed from each other.

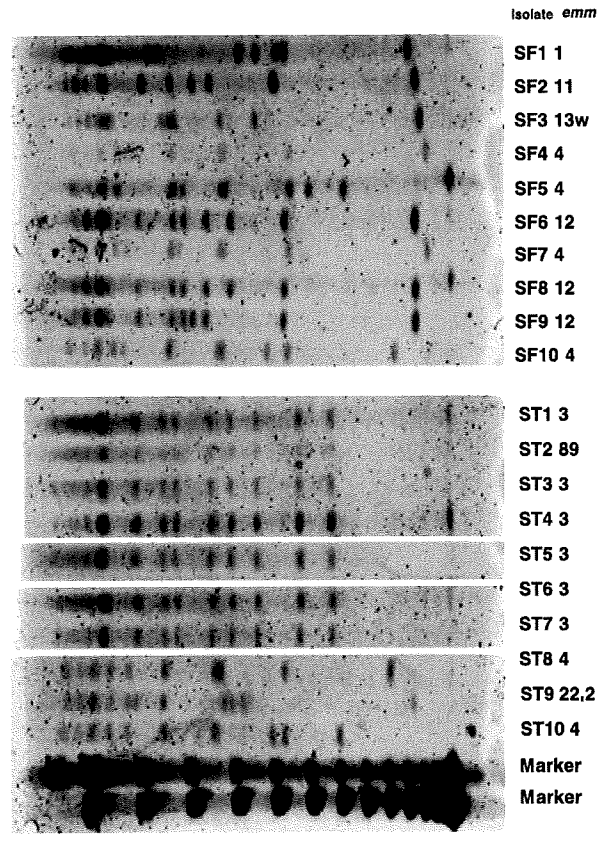

Fig. 1. PFGE patterns of the GAS isolates used in this study. The GAS isolates were digested with SmaI and analyzed by PFGE. The names of the isolates and their *emm* types are shown.